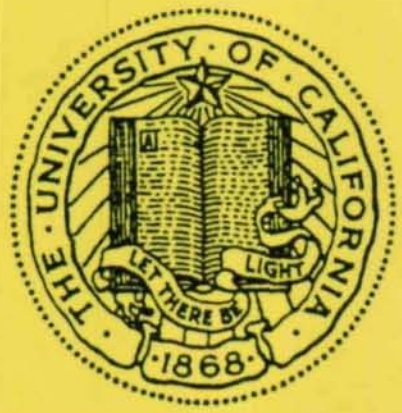

STRUCTURAL SYSTEMS RESEARCH PROJECT

Report No.
SSRP–2001/05

EFFECT OF STRAIGHTENING METHOD ON THE CYCLIC BEHAVIOR OF k AREA IN STEEL ROLLED SHAPES

by

Chia-Ming Uang
Brandon Chi

Final Report on a Research Project Funded by the American Institute of Steel Construction

May 2001

Department of Structural Engineering
University of California, San Diego
La Jolla, California 92093-0085

University of California, San Diego
Department of Structural Engineering
Structural Systems Research Project

Report No. SSRP – 2001/05

Effect of Straightening Method on the Cyclic Behavior of k Area in Steel Rolled Shapes

by

Chia-Ming Uang
Professor of Structural Engineering

Brandon Chi
Graduate Student Researcher

Final Report on a Research Project Funded by the American Institute of Steel Construction

Department of Structural Engineering
University of California, San Diego
La Jolla, California 92093-0085

May 2001

ABSTRACT

The research objective was to evaluate the effect of rotary-straightening on the cyclic behavior of k area in column sections. A total of five full-scale steel moment connections with W14×l76 column and W2l×l66 beam (A992 steel) were tested with the SAC loading protocol. The first three specimens did not use continuity plates and doubler plate; the only variable was the method of straightening of the columns (rotary-straightened, gag-straightened, and non-straightened). To promote the potential for fracture, a 1-inch diameter hole was drilled in the k area at the bottom flange level of the beam. Continuity plates and a doubler plate were used for the last two specimens–one with a rotary-straightened column and another one with a non-straightened column. No attempt was made to avoid welding of the doubler plate and continuity plates in or near the k area

The first three specimens all failed by fracturing of the column flange outside the panel zone at large drift levels. The fracture initiation was caused by the stress concentration in the middle of the beam flange width because no continuity plates were used. Fracture initiated from the hole in the gag-straightened and non-straightened columns, but not the rotary-straightened column. Thus, no clear pattern indicating that rotary-straightening promoted fracture was observed. Brittle fracture occurred in the beam at 6% drift for the last two specimens. The fracture initiated in the weld access hole, which started in the k area of the beam due to stress concentration. To avoid this type of failure, providing a smooth profile for the weld access hole is important.

Although this testing program did not reveal adverse effect created by rotary straightening, material testing conducted by Lehigh researchers clearly showed that the ductility and toughness of the material in the k area were significantly reduced. Therefore, it is prudent that designers follow the AISC Advisory to avoid welding in the k area.

ACKNOWLEDGEMENT

Funding for this research was provided by the American Institute of Steel Construction. Dr. S. Zoruba and Mr. T. Schlafly served as the coordinating manager for this project. The authors would like to thank Mr. R. Ferch, Vice President of Herrick Corporation, for the generous donation of fabrication service for the moment connection test specimens. Drs. J. Fisher and E. Kaufmann at Lehigh University provided material test data contained in Chapter 2.

TABLE OF CONTENTS

LIST OF TABLES

LIST OF FIGURES

1. INTRODUCTION

1.1 Statement of Problem

Incidents of brittle fracture that initiated from the k area of wide flange sections have been reported recently (Tide 2000). One example in seismic applications is the cracking in the column web when the continuity plates (column transverse stiffeners) are welded to the connection region in shop fabrication. The k area is the region extending from about the midpoint of the radius of the fillet into the web approximately 1 to 1.5 inches beyond the point of tangency between the fillet and web (see Figure 1.1).

The majority of rolled steel shapes have been produced in the past two decades from scarp steel in an electric furnace and cast continuously into near shape configuration. Except for heavy sections, these structural shapes are typically straightened by the rotary straightening process in order to bring them into the dimensional tolerance specified in the ASTM standard. The process involves passing a structural shape through a series of rollers placed near the k areas (see Figure 1.2). Cold bending in these areas during the straightening process generally produces cyclic plastic deformations. Strain hardening together with strain aging results in higher tensile strength, lower ductility and toughness (Tide 2000, Jaquess and Frank 1999). If welding is performed in or near the k area, thermal strains are likely to serve as a trigger to promote brittle fracture.

In response to the concerns raised by the designers and fabricators, AISC issued an advisory (Iwankiw 1997), suggesting some interim measures to mitigate the k area problem. In the meantime, AISC also initiated a series of research projects to study the issue. The AISC research includes four studies. The first study, conduced at Lehigh University, deals with the characterization of cyclic inelastic strain behavior on properties of rolled sections (Kaufmann et al. 2001). The second study, load tests on the k area of rotary-straightened column sections to determine the effects on performance, was conducted at both Lehigh University (Kaufmann et al. 2001) and the University of California, San Diego (UCSD); the UCSD part deals with seismic moment frame applications. To minimize the effect of welding in the panel zone region, a reassessment of the design criteria and new alternatives for continuity plates and web double plate is

conducted as the third study at the University of Minnesota (Dexter et al. 2001). The fourth study, also conduced at the University of Minnesota, deals with the updating of standard shape material properties database for design and reliability (Dexter et al. 2001).

1.2 Objective of Research

This research was parallel to the pull-plate monotonic tests at the Lehigh University. The objective of the research at UCSD was to investigate experimentally the effect of member straightening methods on the rolled steel column performance in seismic moment-resisting frames.

1.3 Scope

To evaluate the effect of rotary straightening on the cyclic performance of rolled wide-flange shapes, members that were either not straightened or straightened by gag were also included in the experimental program. A total of five full-scale moment connection specimens were tested with the SAC loading protocol. Tensile coupon tests were conducted on the column shapes. More thorough material testing of the column shapes, showing the effect of rotary straightening on the material characteristics in the k area, was conducted at Lehigh University. (Steel column shapes used for the research at both Lehigh University and UCSD were from the same heat of steel.)

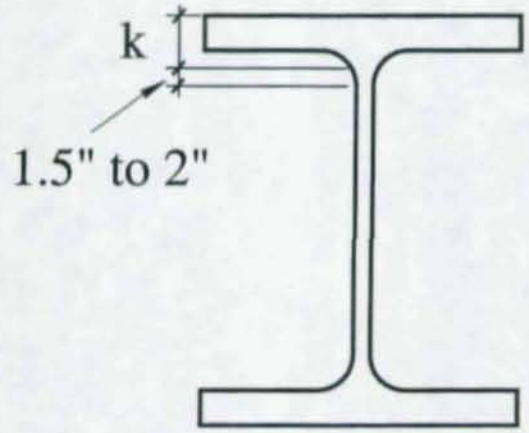

Figure 1.1 k Area in a Wide-flange Section

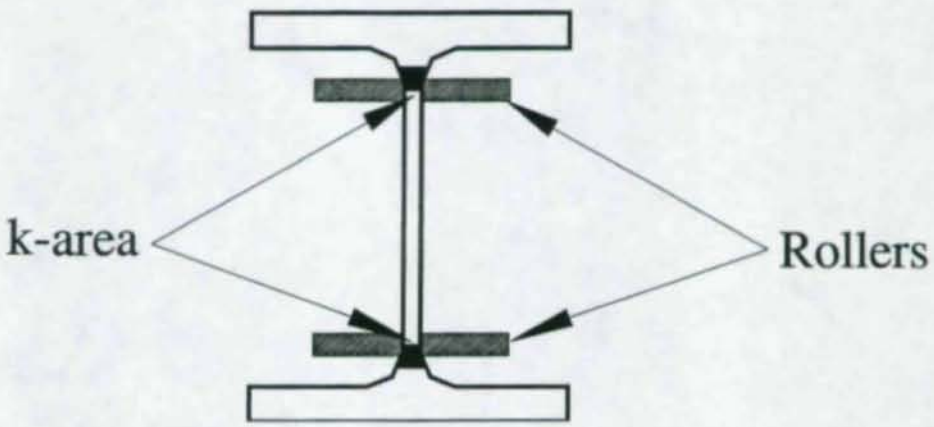

Figure 1.2 Rotary-straightening of Rolled Shape

2. TESTING PROGRAM

2.1 Test Specimens

Figure 2.4 shows the test setup that is commonly used for the cyclic testing of steel moment connections. The column and beam seizes for all five specimens were W14×176 and W21×166, respectively; A992 steel was specified. The column shapes for both the Lehigh and UCSD specimens were from the same heat (Heat No. 150314 from Nucor-Yamato).

Table 2.1 shows the test matrix. The first three specimens (Specimens K1 to K3) did not use continuity plates and doubler; the only variable was the method of straightening. Figure 2.5 shows the connection details. The beam was sized to introduce high concentrated forces through flanges to the column without experiencing significant yielding and buckling in the beam. Since the objective of this study was focused on the k area in the column, not the beam flange groove welded joints, these welds were made in the shop. It was specified that shop welding be done with electrodes having a minimum Charpy V-Notch impact value of 20 ft-lbs at -20° F. To promote the likelihood of fracture in the k area such that the relative performance of three columns with different straightening schemes could be studied, a 1-in. diameter drilled hole in the k area, located at the bottom flange level of the beam, was specified. Nevertheless, the as-received specimens showed that these holes were actually drilled because the column web was too thick to punch. It should be noted that the connection was not designed to meet the seismic design provisions. Instead, the design objective was to introduce large concentrated forces to the column.

Continuity plates and a ½-in. thick doubler plate were used for Specimens K4 and K5 (see Figure 2.6). The doubler plate of A36 steel was groove welded to the column web near the k area in an attempt to "disturb" the material property in the k area by the welding heat input.

Fabrication of test specimens was provided by Herrick Corporation.

2.2 Material Characteristics

Table 2.2 shows the chemical analysis of the steels as obtained from the certified mill test reports. Steel coupons were cut from the column web and column flange for tensile testing at UCSD. The measured mechanical characteristics are presented Table 2.3.

More thorough tensile tests of the coupons taken from the column flange, web, and k area were conducted at Lehigh University (Kaufmann et al. 2001); the locations of the coupons are shown in Figure 2.1, and the results are listed in Table 2.4. Note that the yield strength of the coupons taken from the k area of the rotary-straightened member was much higher than those of the other coupons. Rotary straightening also significantly reduced the elongation, which is a measure of material ductility, from about 30% to 10%. However, such increase in yield strength reduction in elongation did not exist for the gag-straightened member. A comparison of the stress versus strain curves for the coupons taken from the k areas is presented in Figure 2.2

Hardness and Charpy V-Notch (CVN) tests were also conducted by Lehigh researchers. The variations of the measured values in Figure 2.3 clearly show that rotary-straightening significantly reduced the toughness in the k area.

2.3 Specimen Design

2.3.1 Specimen K1 to K3

According to Formula (K1-1) of the LRFD Specification (AISC 1994), the strength for the limit state of local flange bending of the column is

$$R_n = 6.25 t_f^2 F_{yf} = 6.25(1.31)^2(50.0) = 536 \text{ kips} \quad (2.1)$$

where the measured yield strength of the column flange is used for F_{yf}. The strength for the limit state of local web yielding of the column, as given by Formula (K1-2) of the LRFD Specification, is

$$R_n = (5k + N)F_{yw}t_w = (5\times 2.0 + 1.36)(52.0)(0.83) = 490 \text{ kips} \quad (2.2)$$

where F_{yw} is the measured yield strength of the column web. Therefore, local web yielding governs the strength.

A beam size of W21×166 was selected such that the beam will remain essentially elastic while supplying a sufficient amount of concentrated force to the column flange. Assuming that the beam remains elastic and that beam theory can be applied to compute the bending stress in the beam flange, it can be shown that the beam flange force, P_f, at the column face is related to the applied load, P, as follows:

$$P_f = \frac{PL_b(d - t_f)b_f t_f}{2I_x} = 6.4P \tag{2.3}$$

where L_b is the distance from the loading point to the column face. Equating Eqs. 2.2 and 2.3 give a P value when the web local yield strength is reached:

$$P_{LWY} = \frac{490}{6.4} = 76.6 \text{ kips} \tag{2.4}$$

The panel zone strength based on Formula (9-1) of the AISC Seismic Provisions (AISC 1997) is

$$V = 0.6F_{yc}d_c t_{cw}\left[1 + \frac{3b_{cf}t_{cf}^{\ 2}}{d_b d_c t_{cw}}\right]$$

$$= 0.6(52.0)(15.22)(0.83)\left[1 + \frac{3(15.65)(1.31)^2}{22.48(15.22)0.83}\right] = 506 \text{ kips} \tag{2.5}$$

Note that the panel zone strength in the above equation corresponds to a shear strain level of 4 times the shear yield strain. The relationship between the panel zone shear strength and the applied load is

$$V_{pz} = P_f - V_c = P_f - \frac{PL_c}{H_c} = 6.4P - 1.1P = 5.3P \tag{2.6}$$

where V_c is the column shear force, L_c is the distance from the loading point to the centerline of the column, and H_c is the column height. Equating Eqs. 2.5 and 2.6 gives the applied load when the panel zone shear strength is reached:

$$P_{pz} = \frac{506}{5.3} = 95.5 \text{ kips} \tag{2.7}$$

A comparison of Eqs. 2.4 and 2.7 shows that local web yielding would govern the strength of the test specimens K 1 to K3.

2.3.2 Specimens K4 and K5

Continuity plates are used such that local flange bending and local web yielding are not the governing limit states. A 1/2-inch thick doubler plate was used in Specimens K4 and K5 in order to introduce heat input, by welding, near the k area. The panel zone strength is thus increased to

$$V = 506 + 0.6(47.0)(15.22)(0.5)\left[1 + \frac{3(15.65)(1.31)^2}{22.48(15.22)0.5}\right] = 506 + 316 = 822 \text{ kips} \quad (2.8)$$

Lacking coupon test results, the yield strength of the A36 doubler plate is assumed to be 47 ksi (Brockenbrough 2001). Equating Eqs. 2.6 and 2.8 gives the applied load when the panel zone shear strength is reached:

$$P_{px} = \frac{822}{5.3} = 155.1 \text{ kips} \quad (2.9)$$

Therefore, the strength of test specimens K4 and K5 is expected to be 53% stronger than the first three specimens.

The strong column-weak beam condition is satisfied for all test specimens:

$$\frac{\sum M^*_{pc}}{\sum M^*_{pb}} \approx \frac{2Z_c F_{yc}}{Z_b F_{yb}} = \frac{2(320)(50)}{432(50)} = 1.48 \geq 1.0 \quad \text{(OK)} \quad (2.10)$$

2.4 Test Setup

Figure 2.4 shows the test setup. Each specimen was mounted to the strong floor and the strong wall. To simulate inflection points, the ends of the column were mounted on short W14×370 sections, positioned to experience weak-axis bending. A corbel was bolted to the free end of the beam and attached to a servo-controlled actuator. Lateral support for the assembly was provided by a steel column on each side of the beam near the actuator. The two steel columns were tied together with threaded rods to increase lateral stiffness. Greased steel plates attached to the support columns were used to minimize friction between the support column and the beam.

2.5 Test Procedure

Specimen loading followed the SAC standard loading protocol (Clark et al. 1997). The loading sequence is presented in Figure 2.7. The loading sequence was controlled by story drift angle. The loading began with six cycles each at 0.375%, 0.5%, and 0.75% drift. The next four cycles in the loading sequence were at 1% drift, followed by two cycles each at 2%, 3%, 4%, etc., until the specimen fails. Positive drift was defined as the downward displacement negative bending to the beam.

2.6 Instrumentation

The instrumentation included the use of strain gages, rosettes, and displacement transducers. Figure 2.8 shows the location of the displacement transducers for monitoring the global response of the first three specimens. Displacement transducers L2, L3 were placed diagonally in the column web panel zone to monitor the average shear deformation. Transducers L4 and L5 measured the column movement at the beam flange levels, while L6, L7, and L8 monitored column end movement, if any. L9 was used to measure the relative deformation of the column flanges at the top flange level of the beam. L1, used to control the loading sequence, measured the overall vertical displacement at the beam tip. The applied load was measured with a load cell mounted on the actuator. Carefully arranged strain gages and rosettes, as shown in Figure 2.9, were used to measure local responses. Similar arrangements for the displacement transducers, strain gages, and rosettes for Specimens K4 and K5 are presented in Figure 2.10 and Figure 2.11.

2.7 Data Reduction

The data reduction procedure was formulated by Uang and Bondad (1996). The total plastic rotation of the connection was calculated by dividing the plastic component of the beam tip displacement by the length from the tip of the beam to the column centerline.

Table 2.1 Test Matrix

Specimen No.	Straightening Method	Continuity Plates, Doubler Plate
K1	Rotary	No
K2	Gag	No
K3	None	No
K4	Rotary	Yes
K5	None	Yes

Table 2.2 Chemical Compositions

Specimen	Member	Heat No.	C	Mn	P	S	Si	Cu	Ni	Cr	CE
Columns	W14×176	150314	0.06	1.34	0.015	0.021	0.24	0.34	0.10	0.11	0.35
Beams	W21×166	154423	0.06	1.10	0.015	0.033	0.24	0.37	0.12	0.07	0.29

$$CE = C + \frac{Mn + Si}{6} + \frac{Cr + Mo + V}{5} + \frac{Ni + Cu}{15}$$

Table 2.3 Beam and Column Mechanical Properties

Member	Coupon	Yield Strength (ksi)	Tensile Strength (ksi)	Elongation* (%)
Column W14×176	Flange	50.0	66.7	33
	Web	52.0	70.5	31
	(Mill Cert.)	(58)	(76)	(21)
Beam W21×166	(Mill Cert.)	(50.0)	(74.0)	(22)

* Based on 8-inch gage length.

Table 2.4 Column Mechanical Properties (Kaufmann et al. 2001)

W14×176	Test Location	Yield Strength (ksi)	Tensile Strength (ksi)	Elongation* (%)
Rotary Straightened	Web	54.14	70.34	29.7
	k-area	77.13, 82.41	85.64, 84.86	9.4, 9.4
	Flange	54.01	70.89	31.3
Gag Straightened	Web	55.06	70.39	28.9
	k-area	52.15, 53.00	69.92, 71.04	29.7
	Flange	53.92	70.99	28.9
Non Straightened	Web	56.03	71.22	28.8
	k-area	54.18, 54.09	71.44, 70.78	29.4, 30.1
	Flange	54.92	71.87	31.3

* Based on 8-inch gage length.

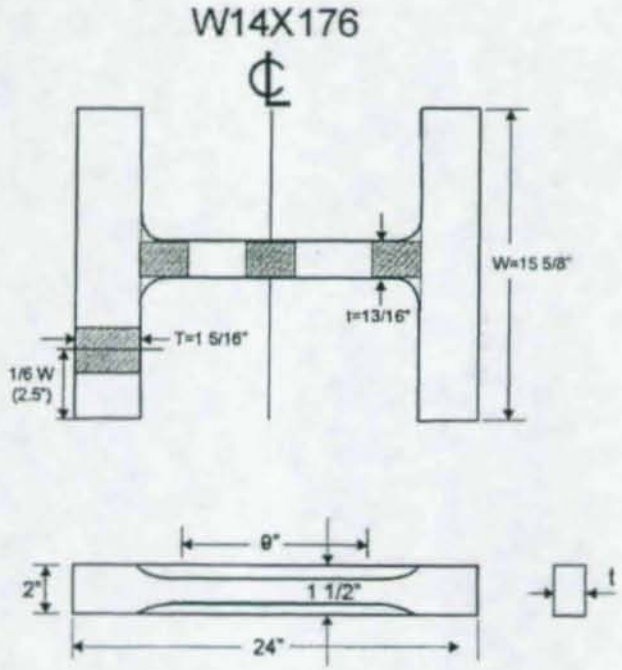

Figure 2.1 Tensile Coupon Layout (Kaufmann et al. 2001)

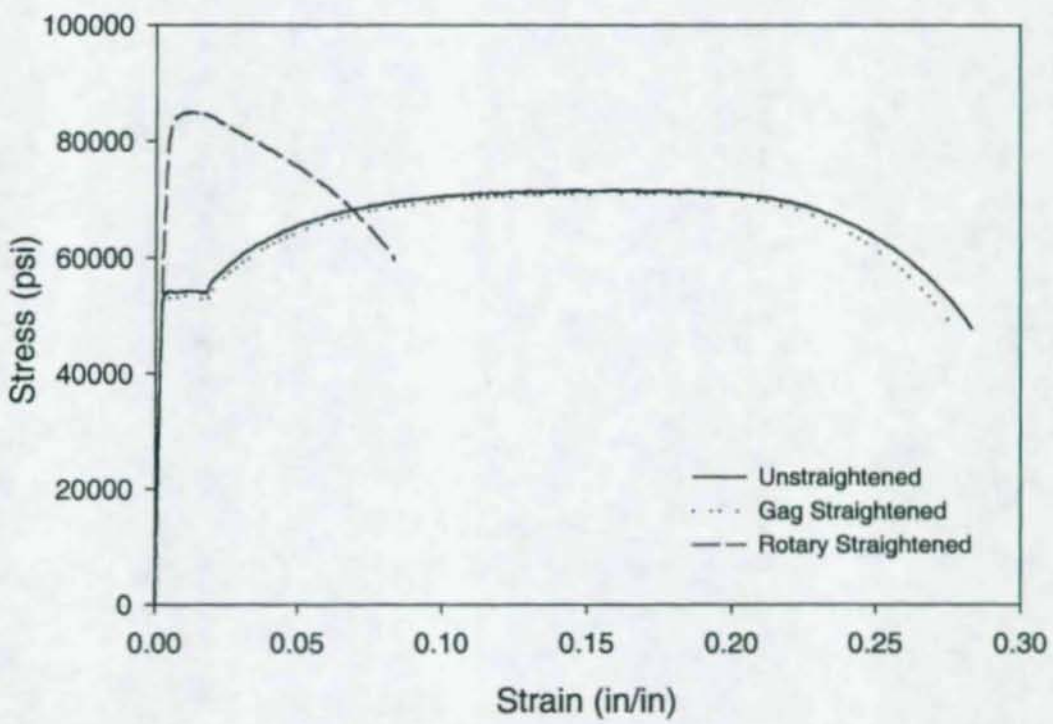

Figure 2.2 k-Area Stress-Strain Behavior for the Three Differently Processed Sections (Kaufmann et al. 2001)

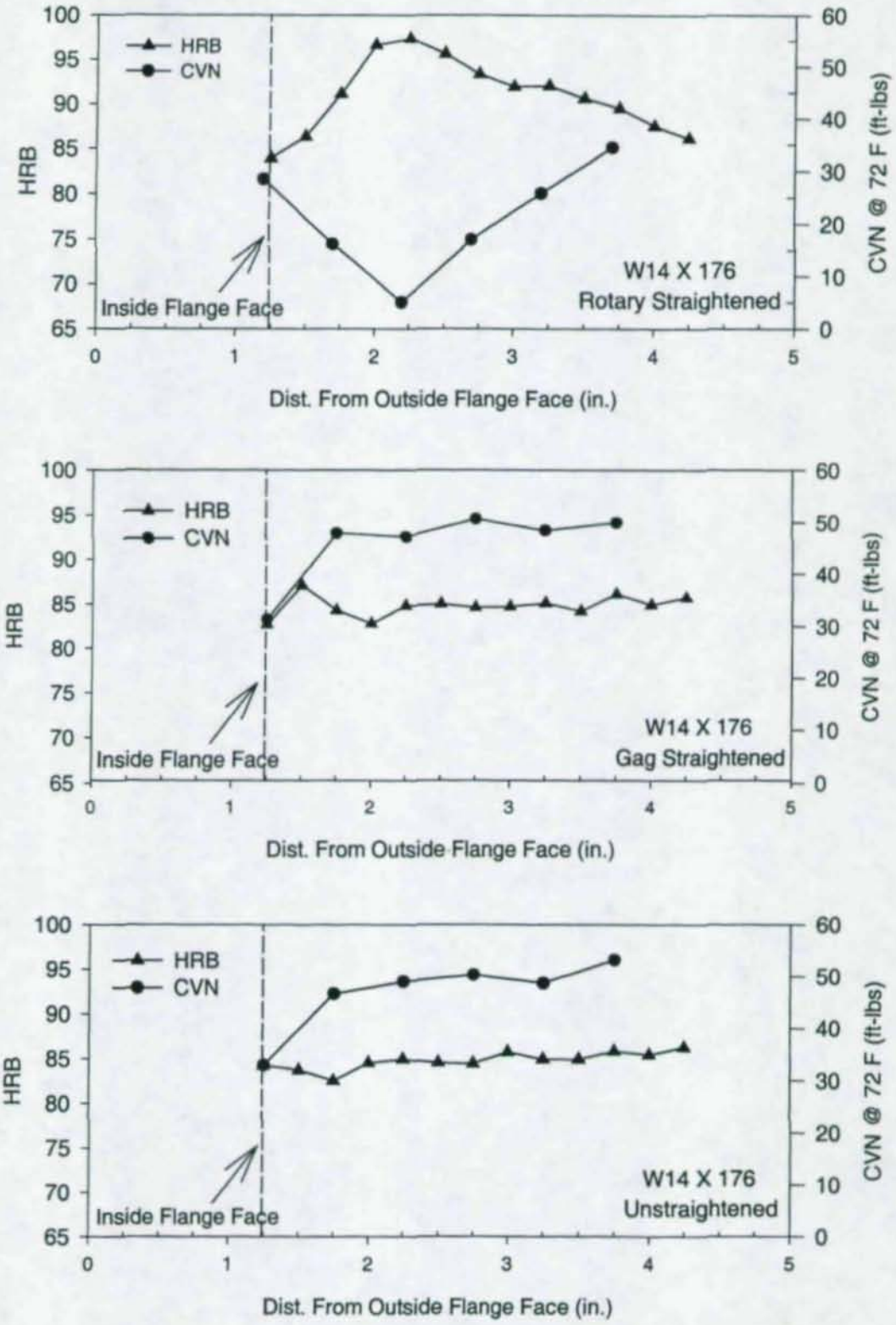

Figure 2.3 k-Area Hardness and CVN for the Three Differently Processed Sections (Kaufmann et al. 2001)

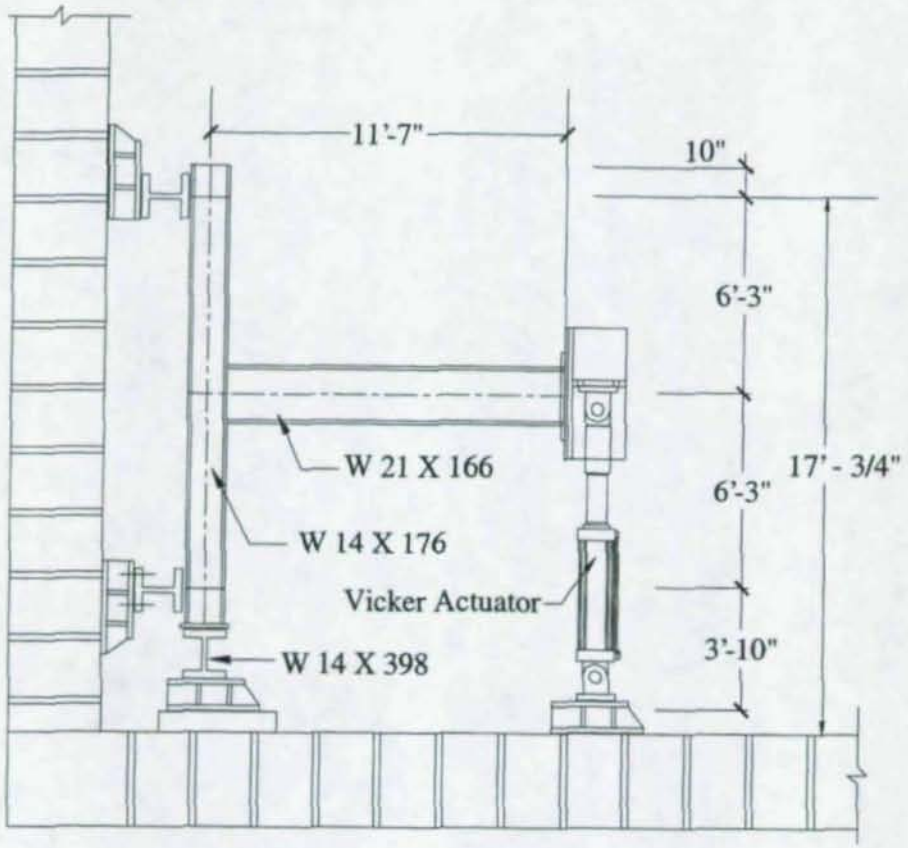

Figure 2.4 Overall Dimensions of Test Assembly

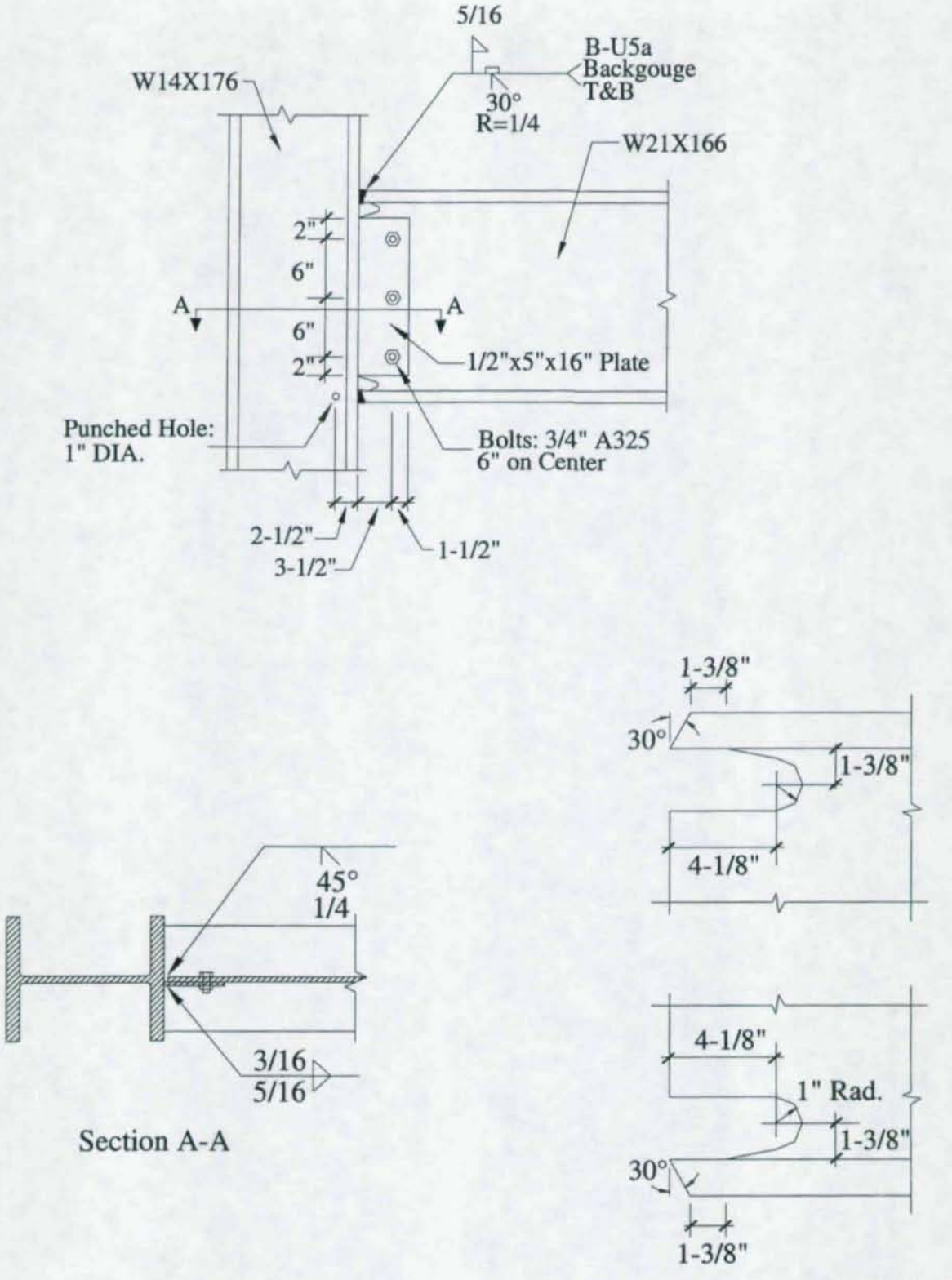

Figure 2.5 Specimens K1 to K3: Moment Connection Details

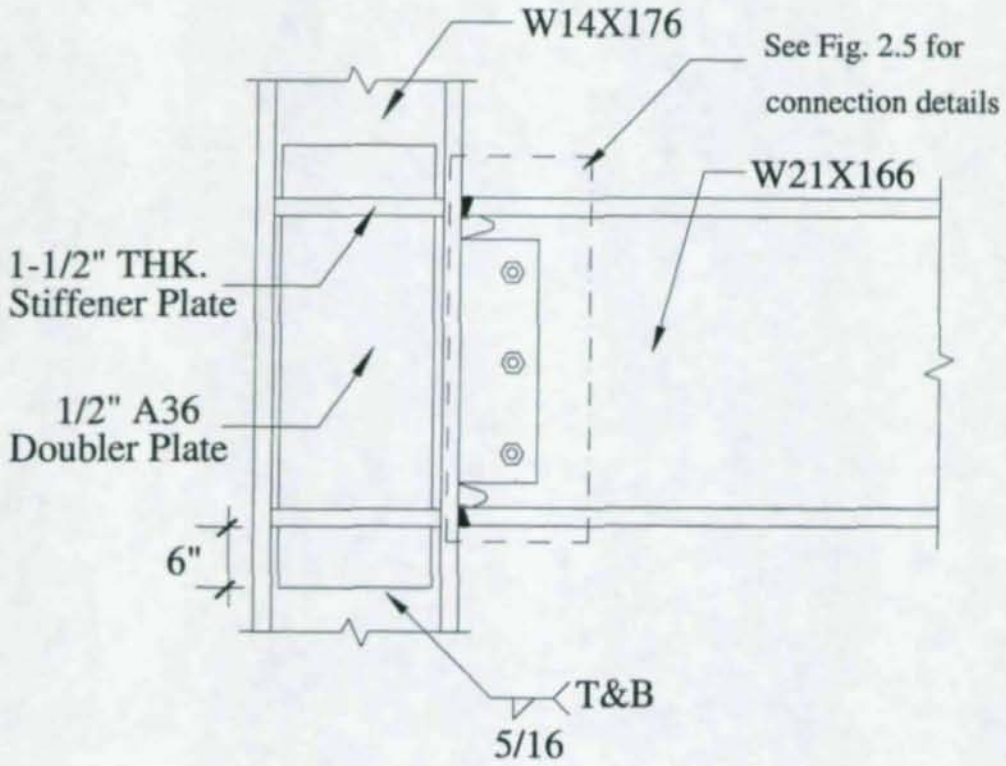

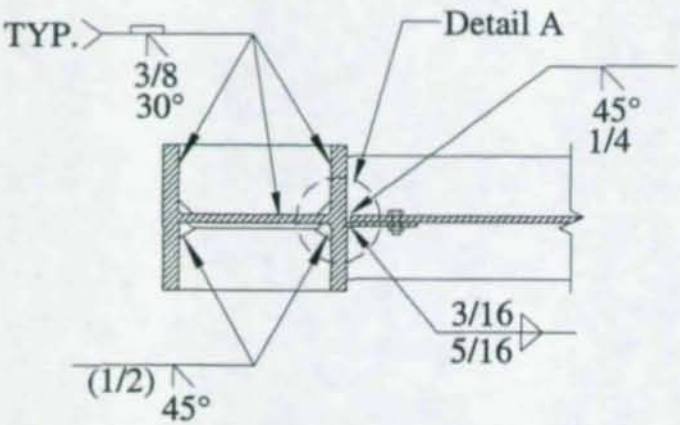

Note: Use A36 steel for doubler plate.

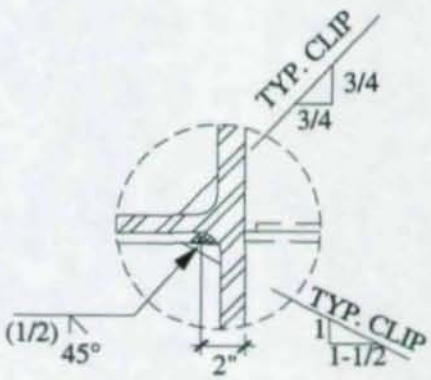

DETAIL A

Figure 2.6 Specimens K4 and K5: Moment Connection Details

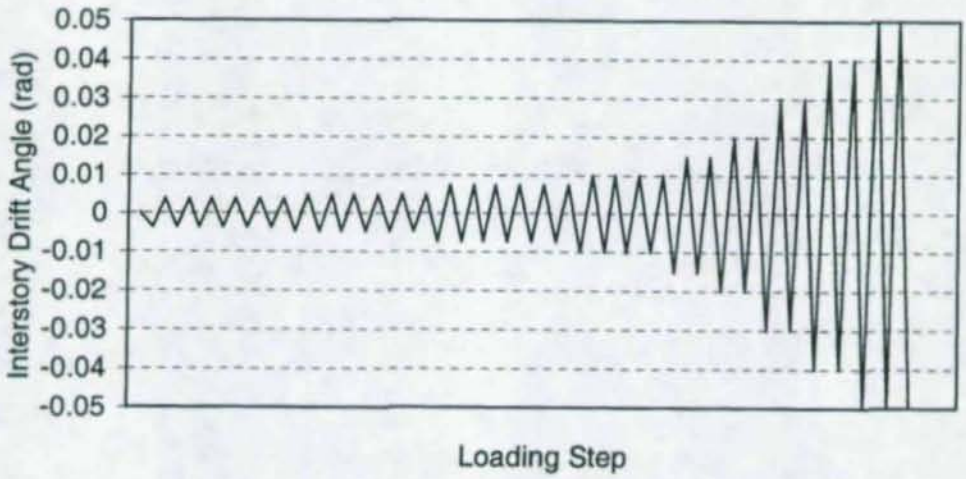

Figure 2.7 SAC Standard Loading History

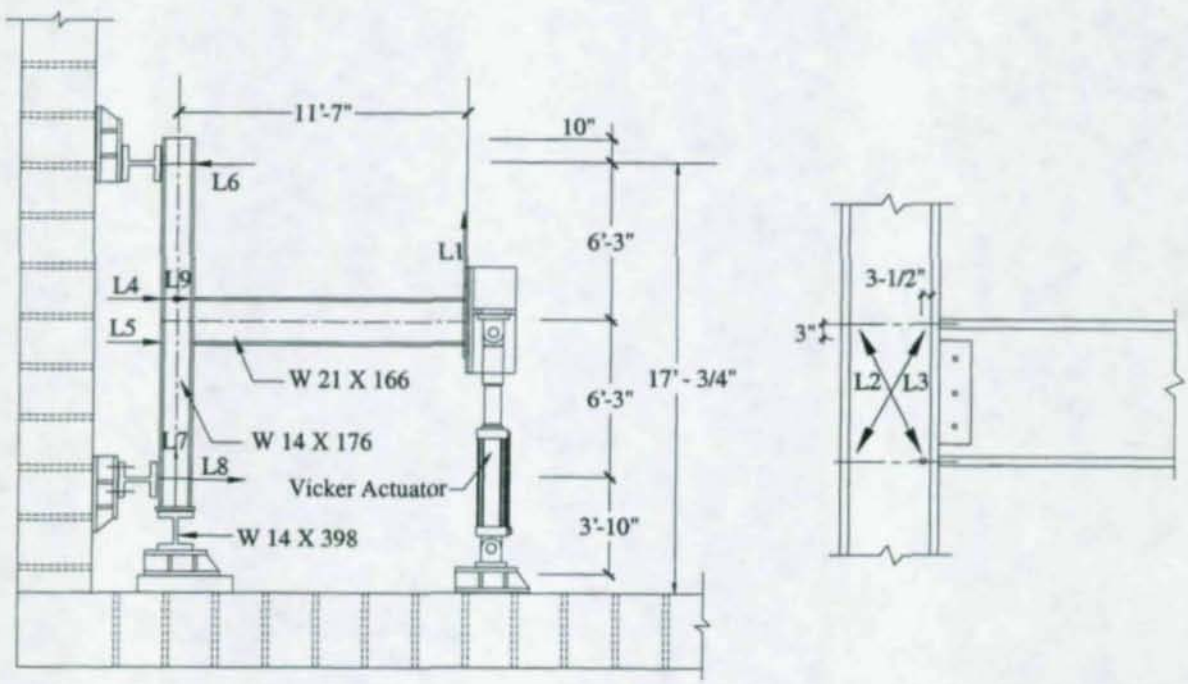

Figure 2.8 Specimens K1 to K3: Layout of Displacement Transducers

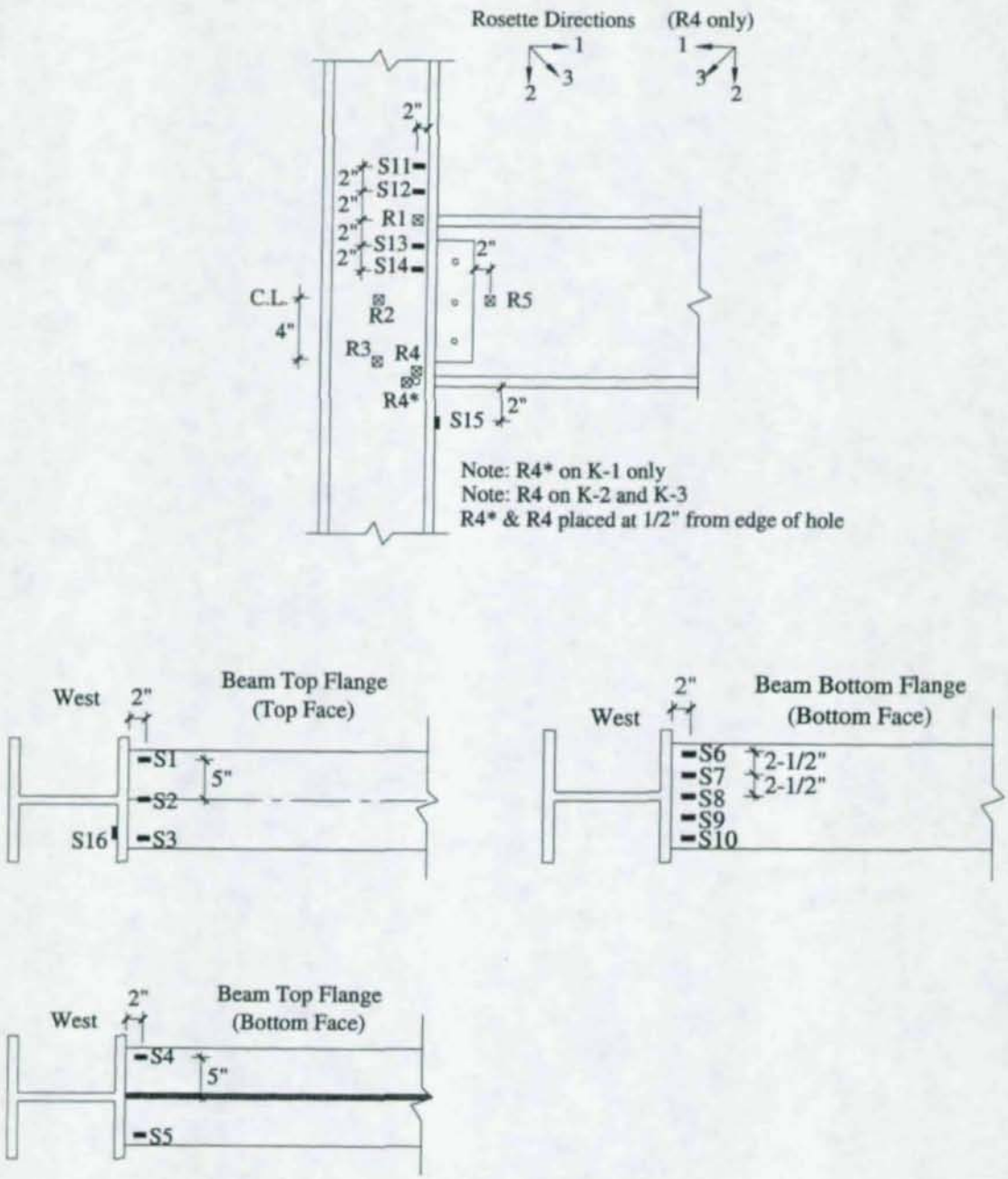

Figure 2.9 Specimens K1 to K3: Strain Gage and Rosette Locations

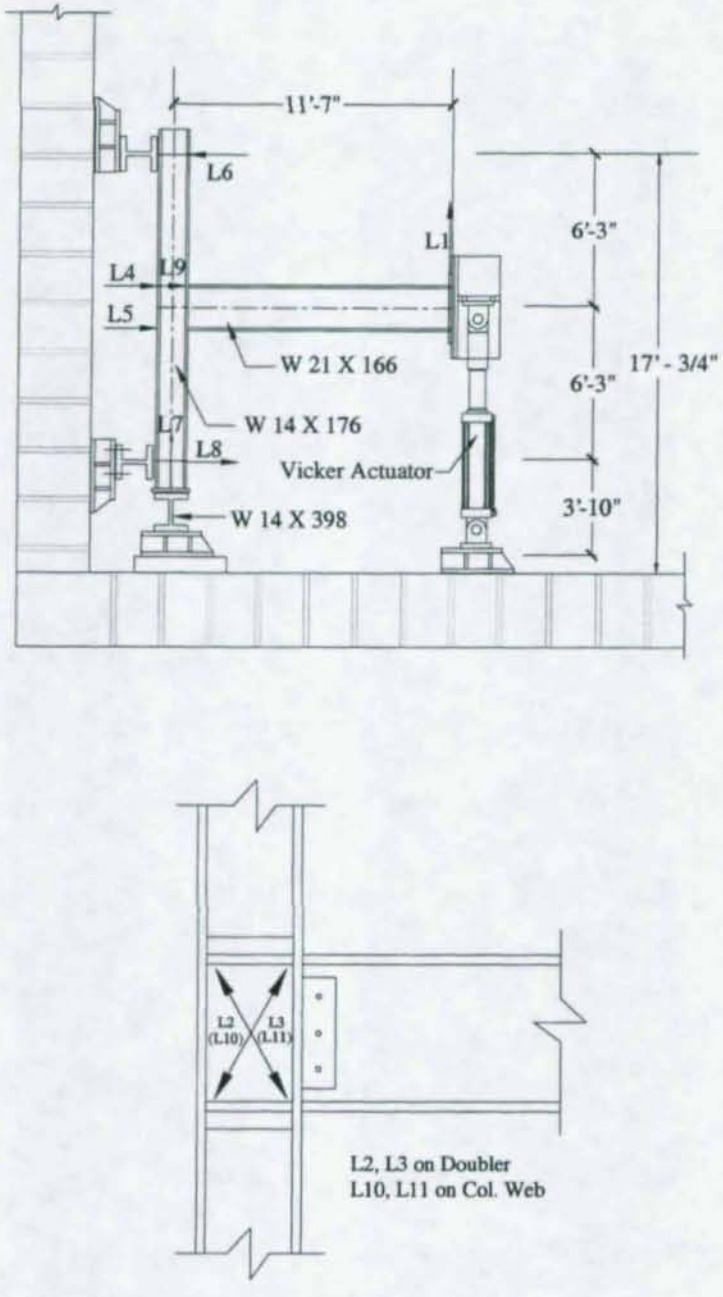

Figure 2.10 Specimens K4 and K5: Layout of Displacement Transducers

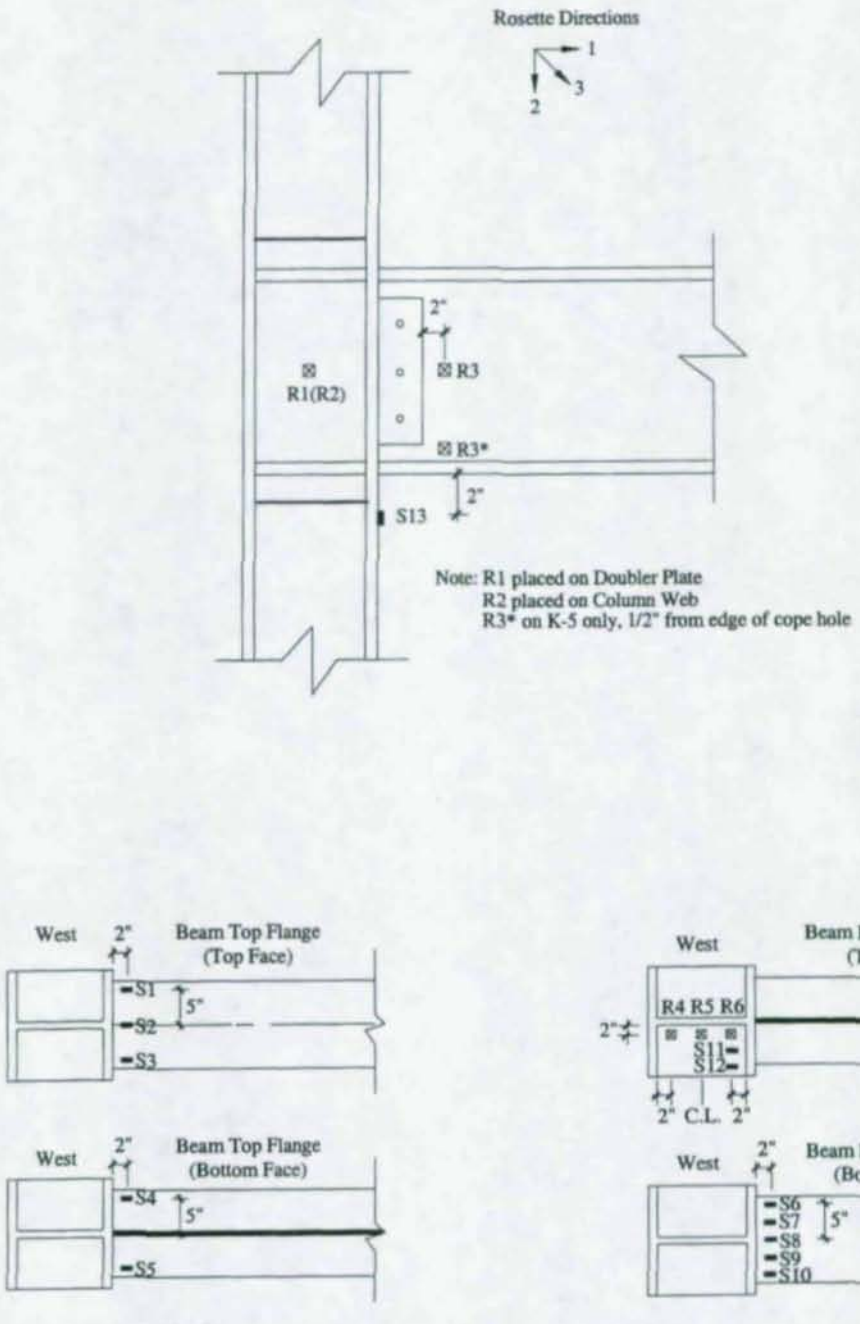

Figure 2.11 Specimens K4 and K5: Strain Gage and Rosette Locations

3. TEST RESULTS OF SPECIMENS WITHOUT CONTINUITY PLATES AND DOUBLER PLATE

3.1 General

Test results of the first three test specimens without continuity plates and doubler plate will be presented in this chapter. For each test specimen, observed performance will be presented first, followed by the recorded global and local responses from displacement transducer and strain gage recordings. The instrumentation plan is shown in Figure 2.8 and Figure 2.9.

3.2 Specimen K1 (Rotary-Straightened Column)

Minor flaking of the whitewash was observed in the panel zone during the 1% drift cycles. At 2% drift, kinking of the column due to panel zone yielding was noticed. Figure 3.1(a) shows the column kinking at 3% drift. Notice the flaking of whitewash in the column flange that occurred just above the top flange and below the bottom flange of the beam. At this drift level, a hairline crack developed at the toe of the groove weld connecting the beam bottom flange to the column flange [see Figure 3.1(b)]. During the first positive excursion of 4% drift, the column flange at the bottom flange level was almost completely fractured [see Figure 3.2(a)]. Figure 3.2(b) shows that the fracture extended into the column web and propagated upward near the k area by about half the beam depth. Before the test was stopped, it was decided to reverse the direction of loading and to displace the beam to 10 in. Figure 3.3 shows the deformed configuration with severe column kinking. Only minor crack at the toe of the top flange groove weld was observed (see Figure 3.4); column fracture at the top flange level could not be developed.

The load versus deflection relationship of the test specimen is shown in Figure 3.5. Discarding the cycle where column fracture occurred, the total plastic rotation reached 0.02 radian (see Figure 3.6).

Strain gages were placed on both faces of the beam top flange, 2 in. away from the column face. A comparison of the readings of a pair of strain gages (S1 and S4, see

Figure 2.9) near one edge of the beam flange is shown in Figure 3.7. Two observations can be made. First, the strain on the outer (top) surface was higher than that on the inner surface. Second, the slopes of both plots are opposite in sign, indicating a significant strain gradient through the thickness of the flange. For example, when the top flange was in tension, the figure indicates that the top face was in tensile strain, while the bottom face was in compressive strain although the strain magnitude was low.

Five strain gages (S6 through S10, see Figure 2.9) were placed across the underside of the bottom flange to monitor strain profiles. Because continuity plates and doubler plate were not used, the strain profiles across the flange width at different drift levels showed significant strain concentration (see Figure 3.8). High strains that occurred in the center of the flange width were responsible for the crack initiation shown in Figure 3.1(b), which eventually led to column fracture.

The column flange tended to bend out of plane (i.e., "warp") because continuity plates were not used; the flaking pattern of the column in Figure 3.2(a) shows this effect. A displacement transducer (L9) was placed at the top flange level of the beam to monitor the relative out-of-plane deformation between two column flanges. Prior to column fracture, the symmetric response in Figure 3.9(a) shows that the deformation was about the same under both tension and compression forces. To measure the amount of transverse strain induced by the out-of-plane bending, a strain gage (S16) was placed transversely on the inside face of the column flange connecting to the beam. Figure 3.9(b) shows that the transverse strain reached the yield strain at 4% drift.

A total of five gages (S11 through S14 and R1) were placed vertically along the k line of the column at the top flange level to monitor the strain profiles (see Figure 3.10). The highest strain reached $24\varepsilon_y$, where ε_y is the actual yield strain, yet no fracture developed in the k area. At the top flange level, the strain state in the column k area is shown in Figure 3.11.

A rosette (R4) was placed above the hole in the k area of the column at the bottom flange level. The response plots shown in Figure 3.12 indicate that the strain levels were not high. Consequently, the rosette was placed to the side of the hole for the next two specimens.

(a) Panel Zone Yielding and Column Kinking

(b) Crack Initiation at Toe of Bottom Flange Groove Weld

Figure 3.1 Specimen K1: Panel Zone Yielding and Crack Initiation at Toe of Bottom Flange Groove Weld (3% Drift)

(a) Fracture of Column Flange

(b) Propagation of Column Fracture near k Area

Figure 3.2 Specimen K1: Fracture of Column Flange at Bottom Flange Level and Propagation near k Area (4% Drift)

Figure 3.3 Specimen K1: Deformed Configuration at 10 in. Beam Deflection

Figure 3.4 Specimen K1: Crack at Toe of Top Flange Groove Weld (10 in. Beam Deflection)

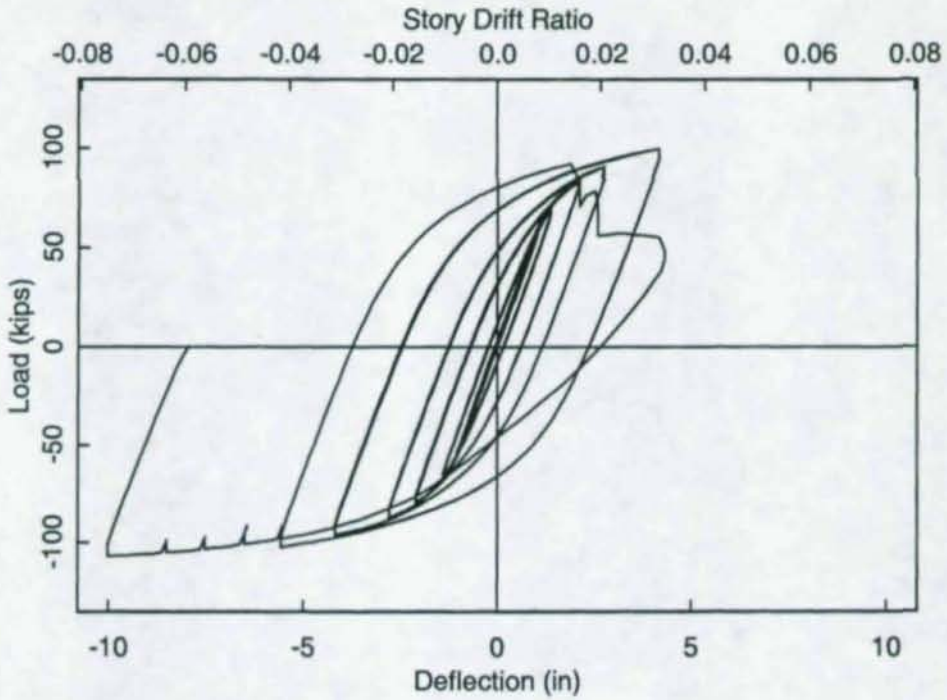

Figure 3.5 Specimen K1: Load versus Beam Tip Displacement Relationship

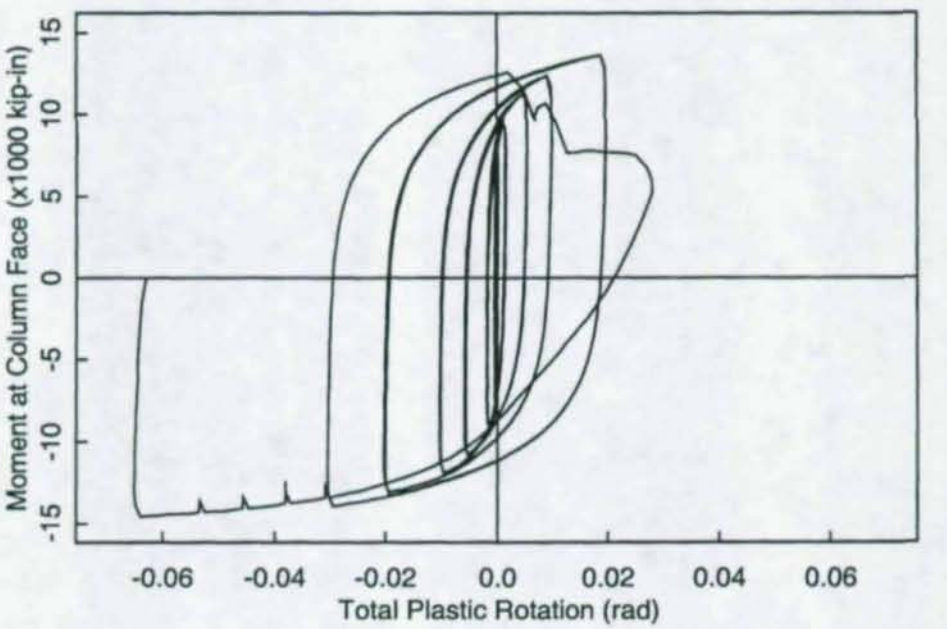

Figure 3.6 Specimen K1: Moment versus Total Plastic Rotation Relationship

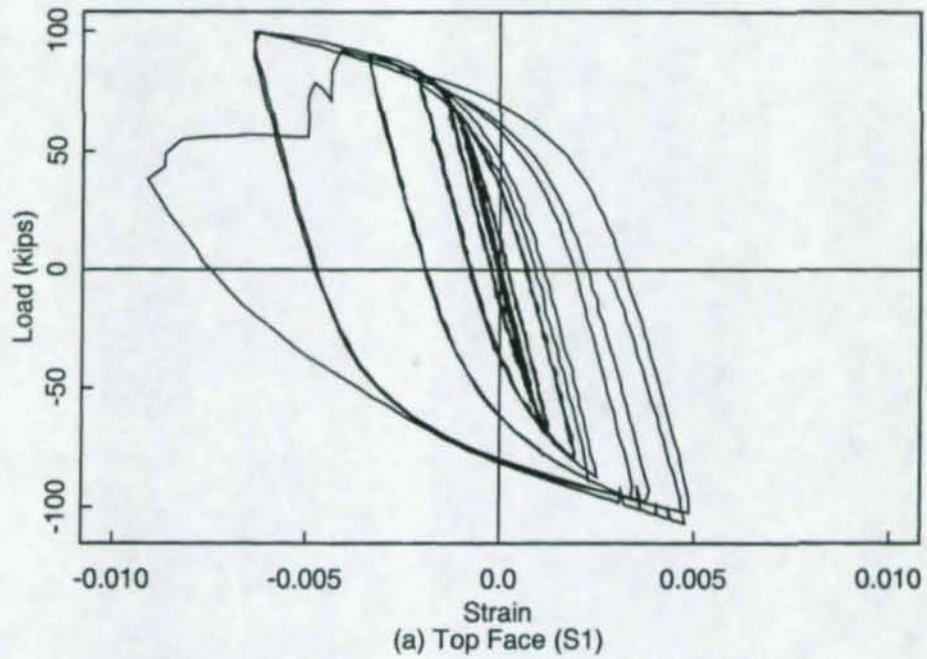

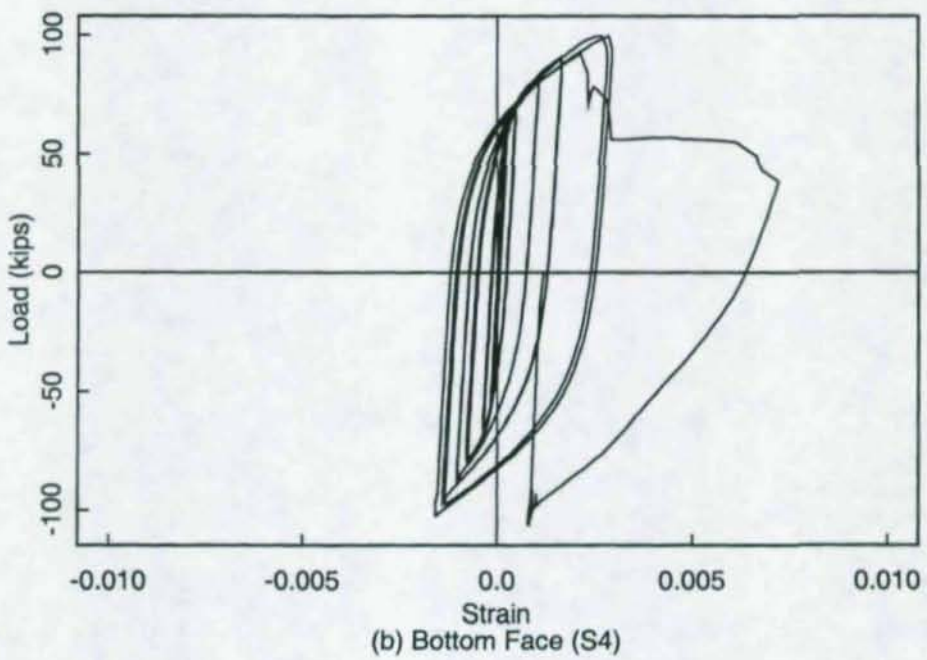

Figure 3.7 Specimen K1: Strain Gradient through Thickness of Beam Top Flange

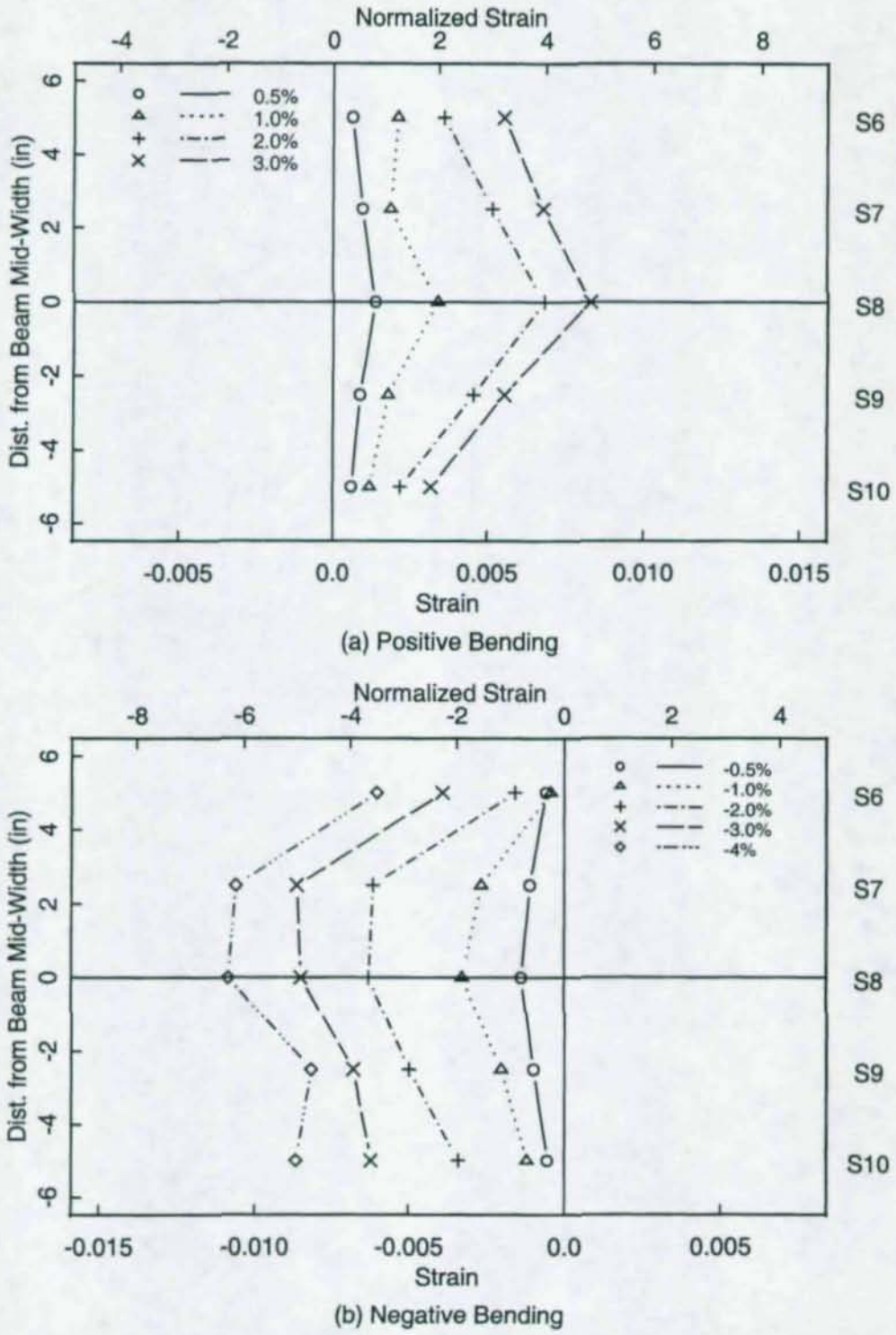

Figure 3.8 Specimen K1: Beam Bottom Flange Strain Profiles

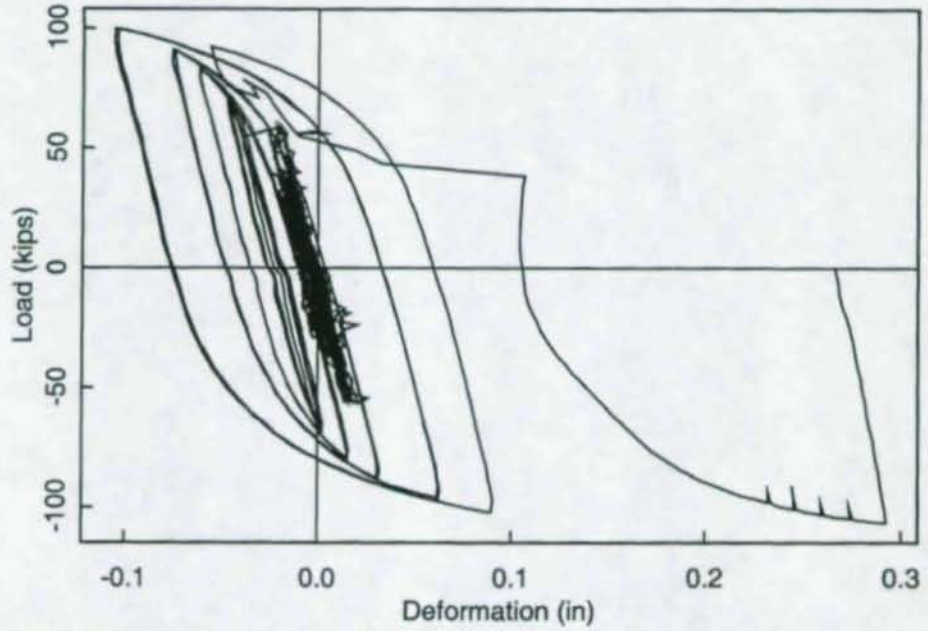

(a) Relative Deformation between Column Flanges

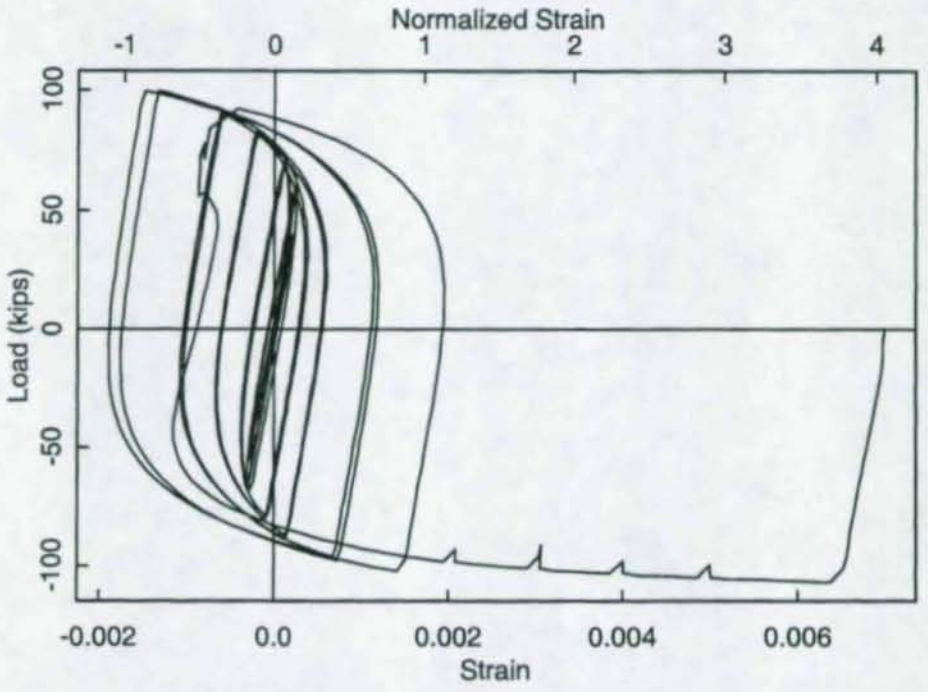

(b) Column Flange Transverse Strain

Figure 3.9 Specimen K1: Response of Column Flange Out-of-plane Deformation and Transverse Strain

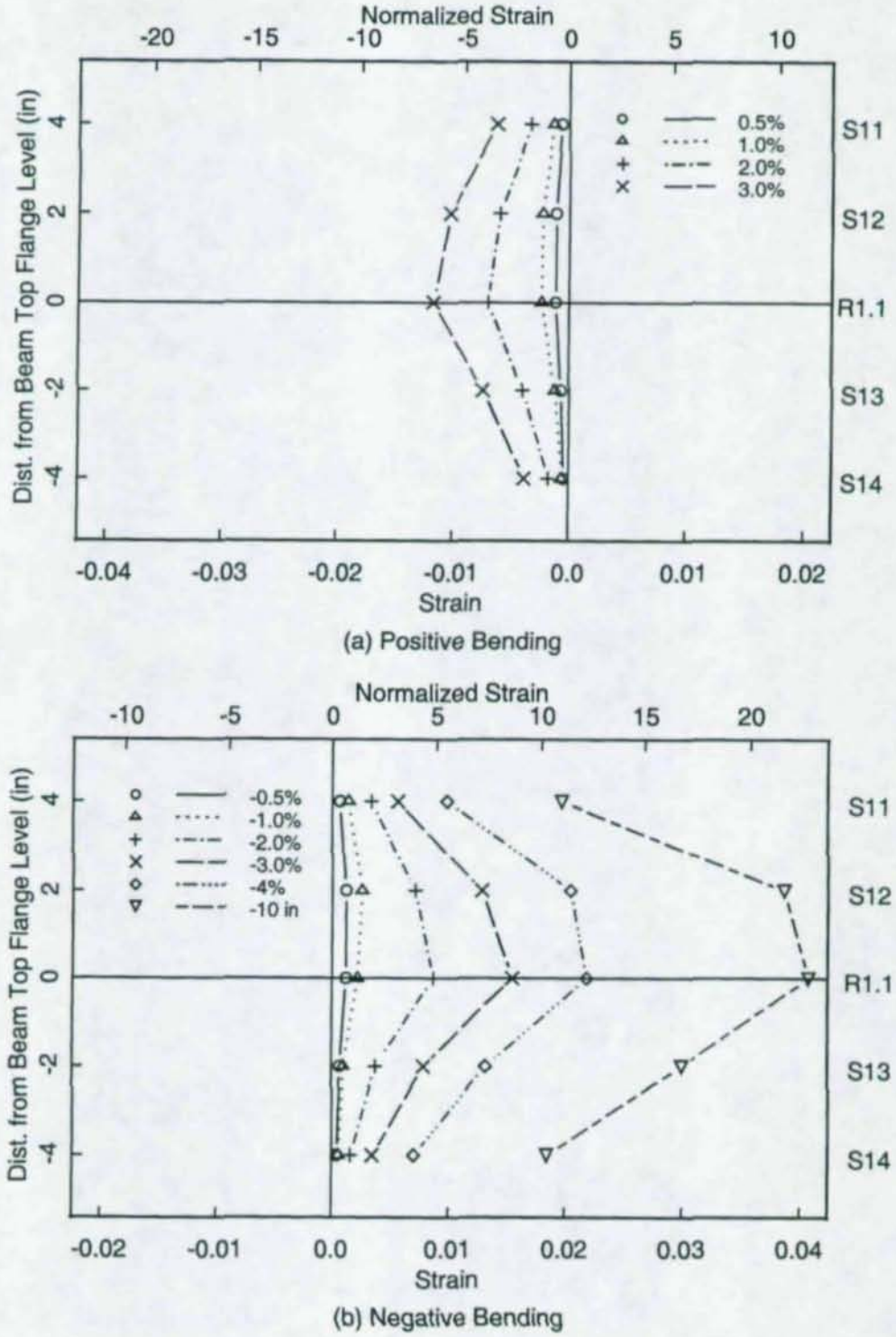

Figure 3.10 Specimen K1: Strain Profiles along Column k Line at Beam Top Flange Level

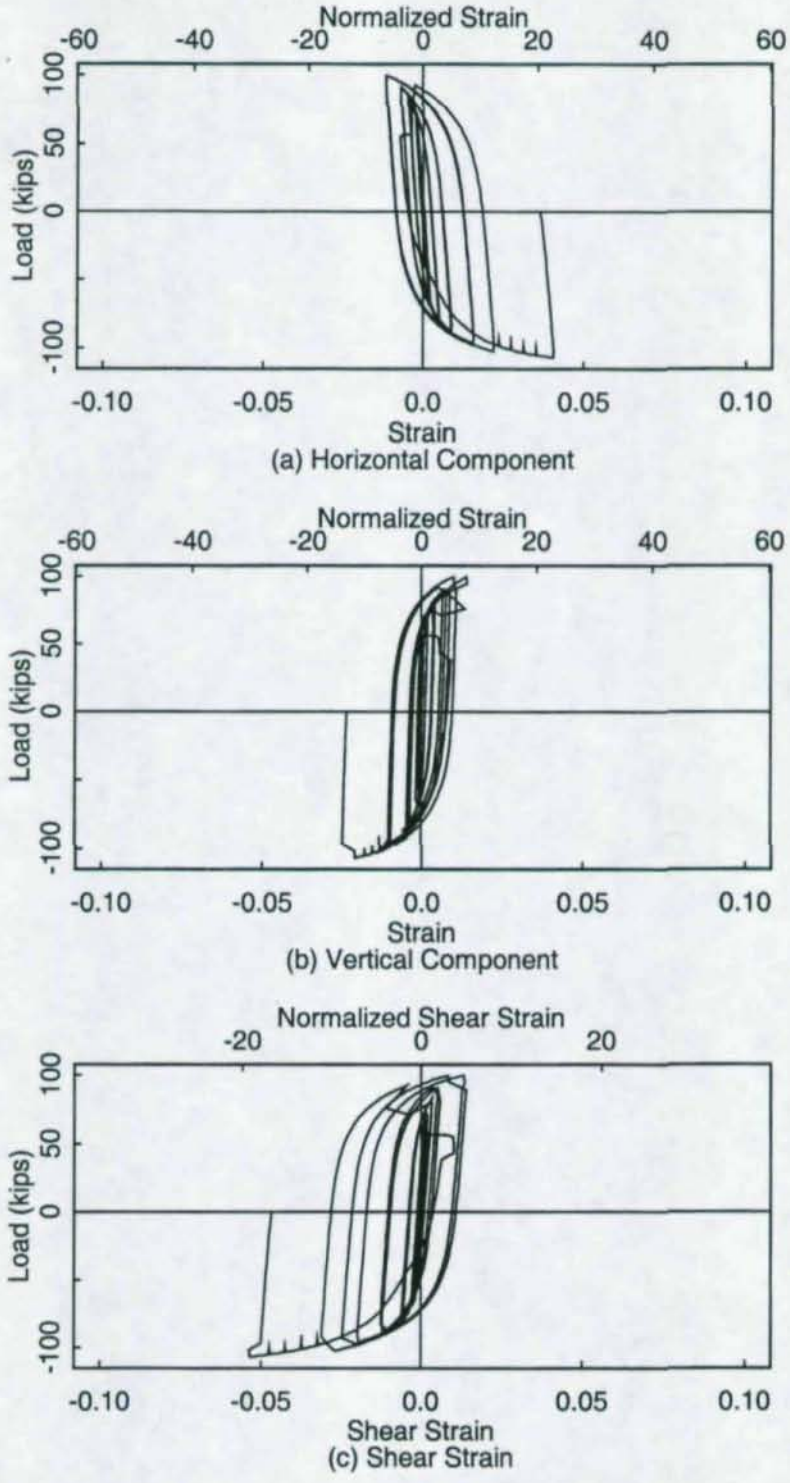

Figure 3.11 Specimen K1: Strains in the Column k Area at Beam Top Flange Level (R1)

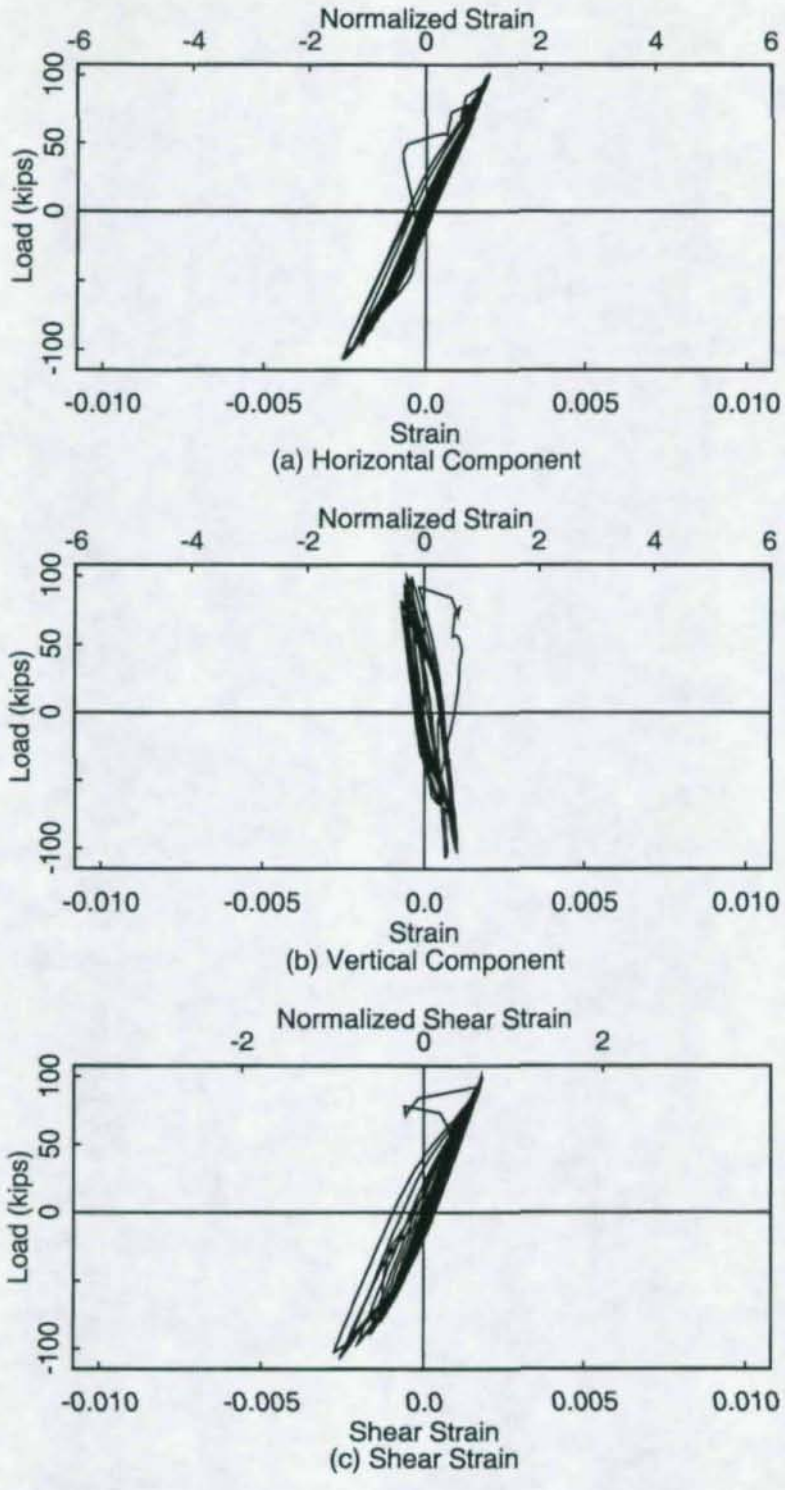

Figure 3.12 Specimen K1: Strains around Hole in the Column k Area Region (R4)

3.3 Specimen K2 (Gag-Straightened Column)

Flaking of the whitewash around the hole, an indication of stress concentration, occurred at 0.5% drift. Flaking in the panel zone was observed at 0.75% drift. Figure 3.13 shows the yielding pattern at 1% drift. Kinking of the column due to panel zone yielding was obvious at 2% drift. At 3% drift level, hair-lines cracks developed at the weld toe of both flanges of the beam. Figure 3.14 shows the extent of crack that propagated into the column flange at the top and bottom flanges at 4% drift. The column flange at the top flange level fractured completely at 5% drift [see Figure 3.15(a)]. Fracture in the column flange also led to a separation in the column web [see Figure 3.15(b)]; the fracture extended into the column web and propagated downward near the k area for about one-fifth of the beam depth. At this point it was decided to reverse the loading direction to test the column at the bottom flange level. Figure 3.16 shows the tearing of the hole at different displacement levels. The fracture propagation was gradual, leading to a slow degradation in strength. The test was stopped at 12 in. beam deflection (8.6% drift). This specimen performed better than Specimen K1. While the latter one was not able to complete one cycle at 4% drift, Specimen K2 was subjected to one complete cycle at 5% drift before the column flange fractured completely.

The load versus deflection relationship of the test specimen is shown in Figure 3.17. Ignoring the incomplete cycle where column fracture occurred, the total plastic rotation reached 0.04 radian (see Figure 3.18).

Strain gradient through the thickness of the beam flange, similar to that shown in Figure 3.7, was also observed in this specimen. Figure 3.19 shows the strain profiles across the width of the beam bottom flange, indicating strain concentration at the mid-width of the beam flange. The out-of-plane deformation of the column flange at the top flange level is shown in Figure 3.20(a). The transverse strain of the column flange in Figure 3.20(b) is lower than that of Specimen K1, probably due to the fracture of the column flange at the beam top flange level. The strain profiles along the k line of the column at the top flange level are depicted in Figure 3.21. The maximum tensile strain reached $12\varepsilon_y$. The strain state in the k area of the column at the top flange level is shown in Figure 3.22. The measured strains next to the hole at the bottom flange level are shown in Figure 3.23.

(a) Yielding Pattern

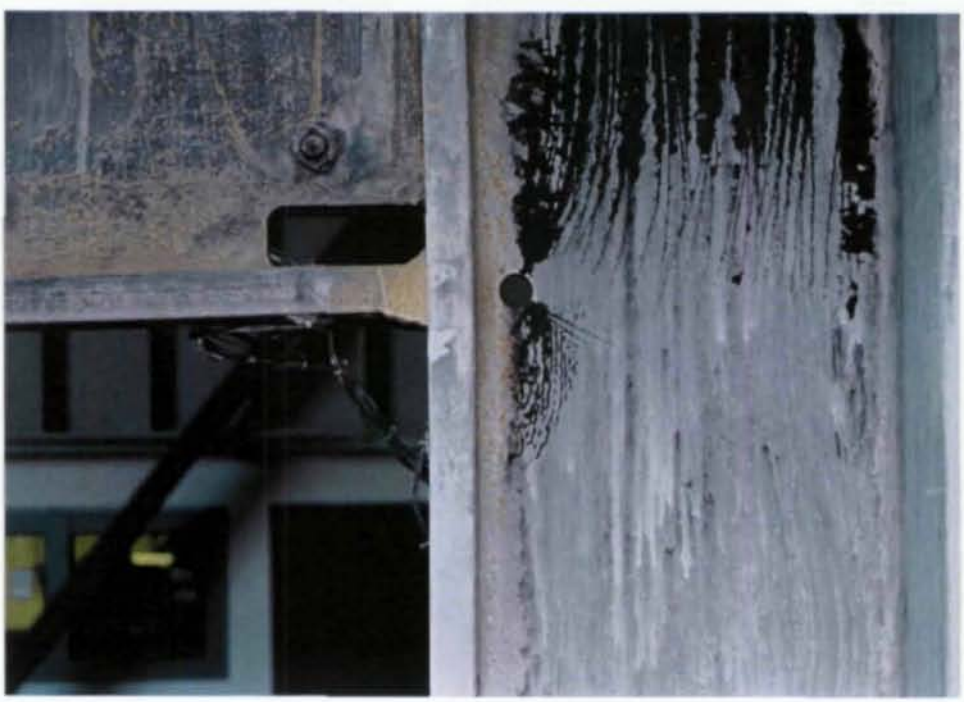

(b) Close-up View

Figure 3.13 Specimen K2: Yielding Pattern (1% Drift)

(a) Top Flange Level

(b) Bottom Flange Level

Figure 3.14 Specimen K2: Fracture of Column Flange (4% Drift)

(a) Fracture of Column Flange

(b) Propagation of Fracture into Column Web near k Area

Figure 3.15 Specimen K2: Fracture of Column at Beam Top Flange Level (5% Drift)

(a) 7 in. Drift

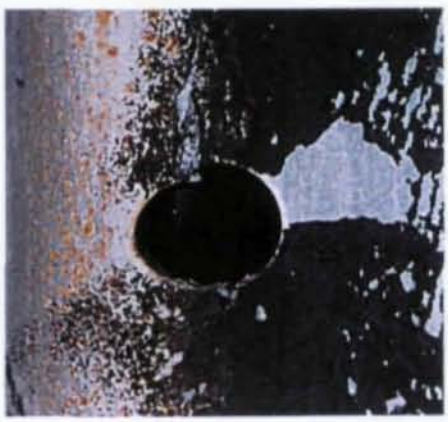

(b) 8 in. Drift

(c) 9 in. Drift

(d) 10 in. Drift

Figure 3.16 Specimen K2: Fracture Propagation in Hole Region

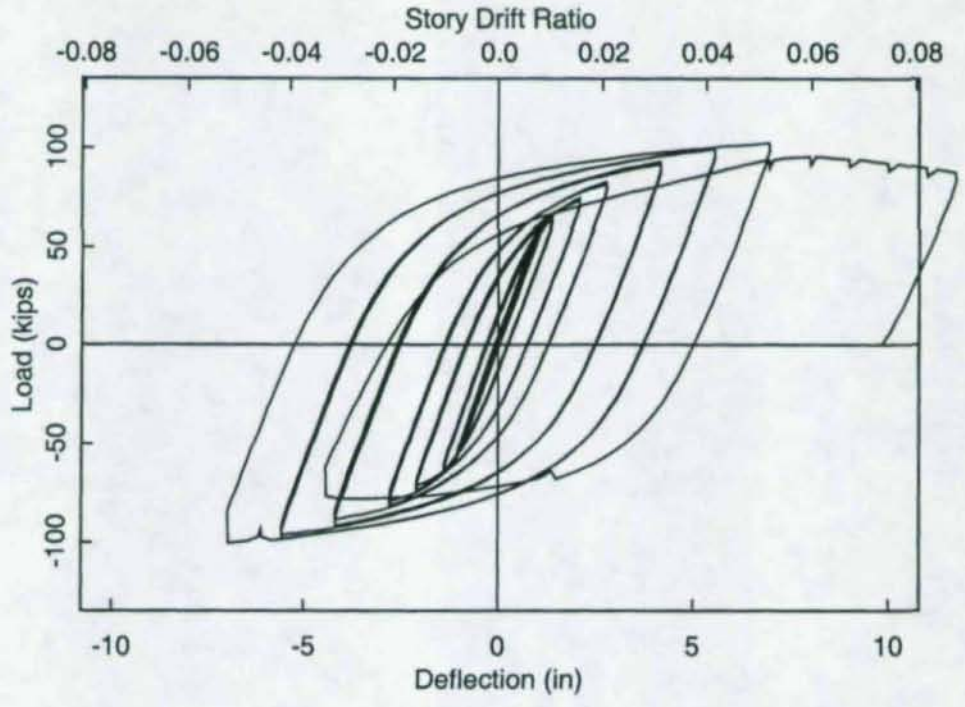

Figure 3.17 Specimen K2: Load versus Beam Tip Deflection Relationship

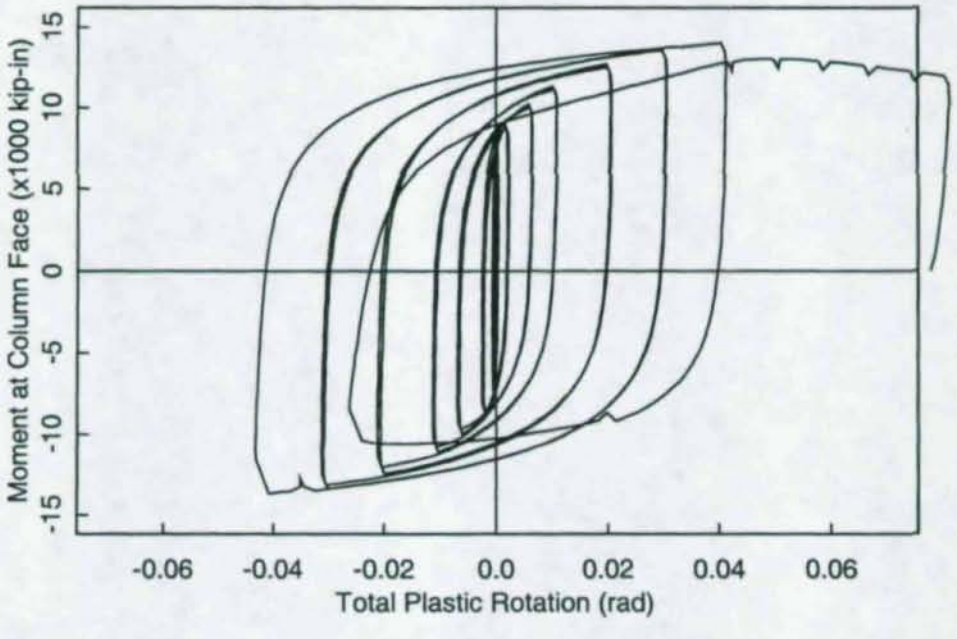

Figure 3.18 Specimen K2: Moment versus Total Plastic Rotation Relationship

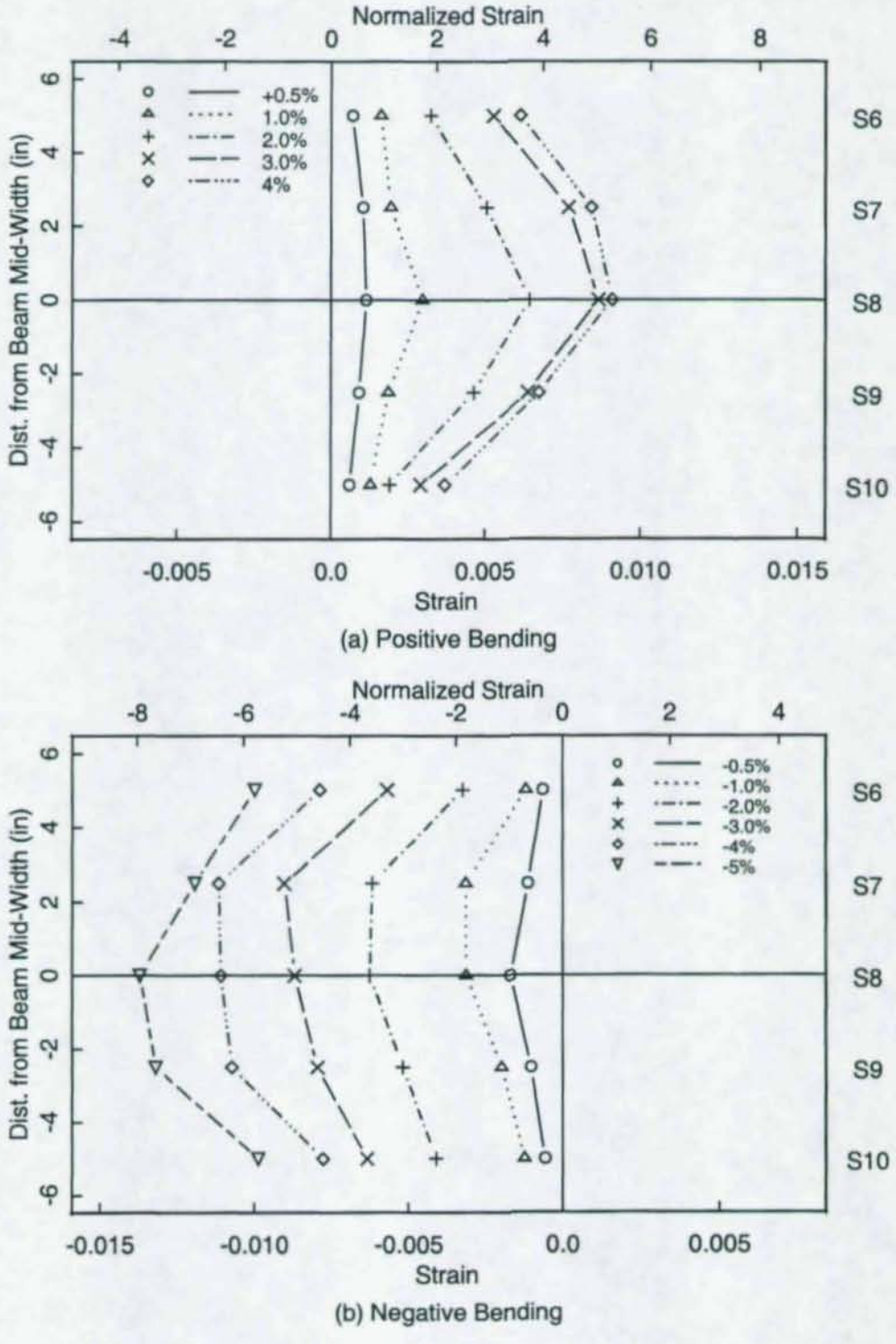

Figure 3.19 Specimen K2: Beam Bottom Flange Strain Profiles

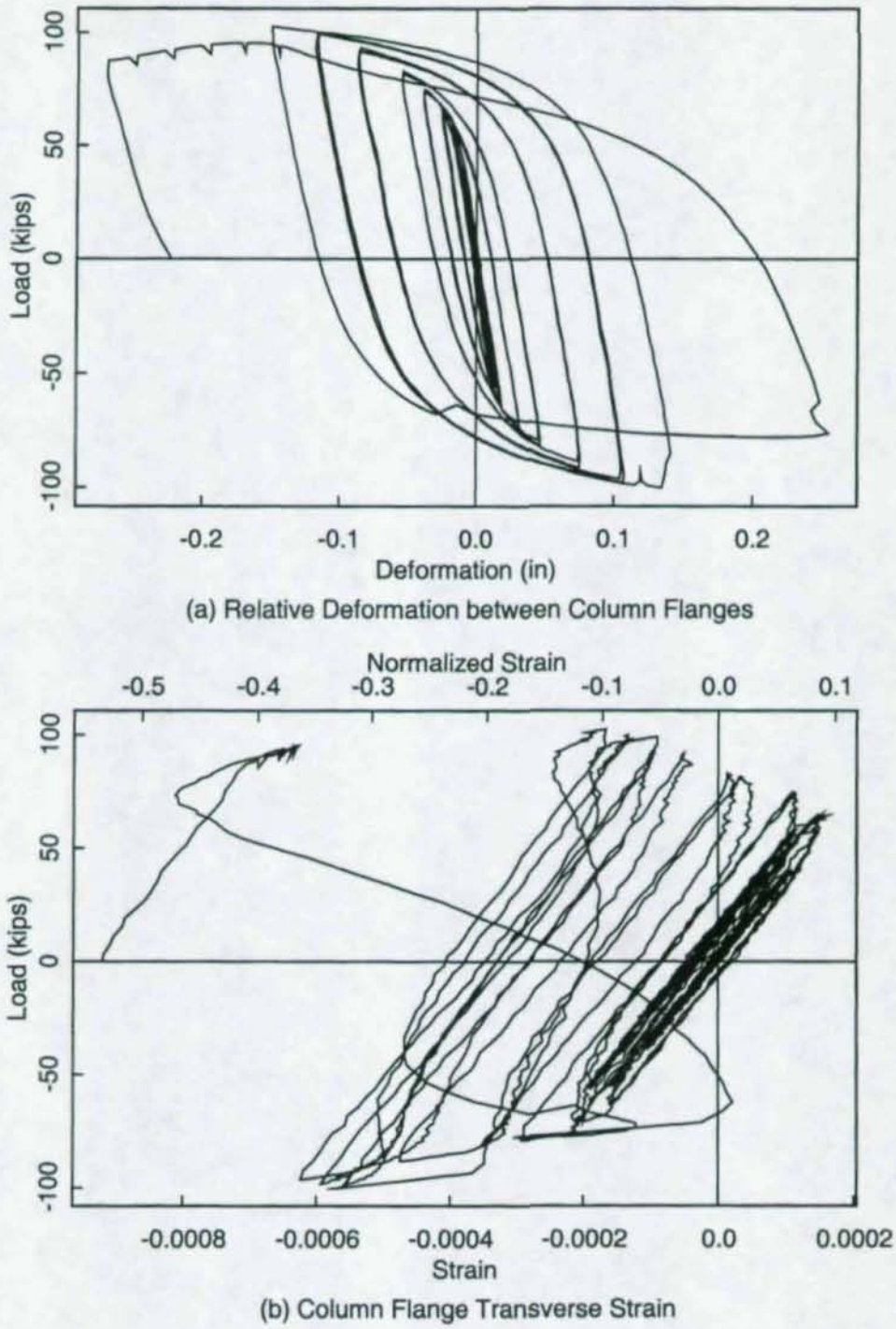

Figure 3.20 Specimen K2: Response of Column Flange Out-of-plane Deformation and Transverse Strain

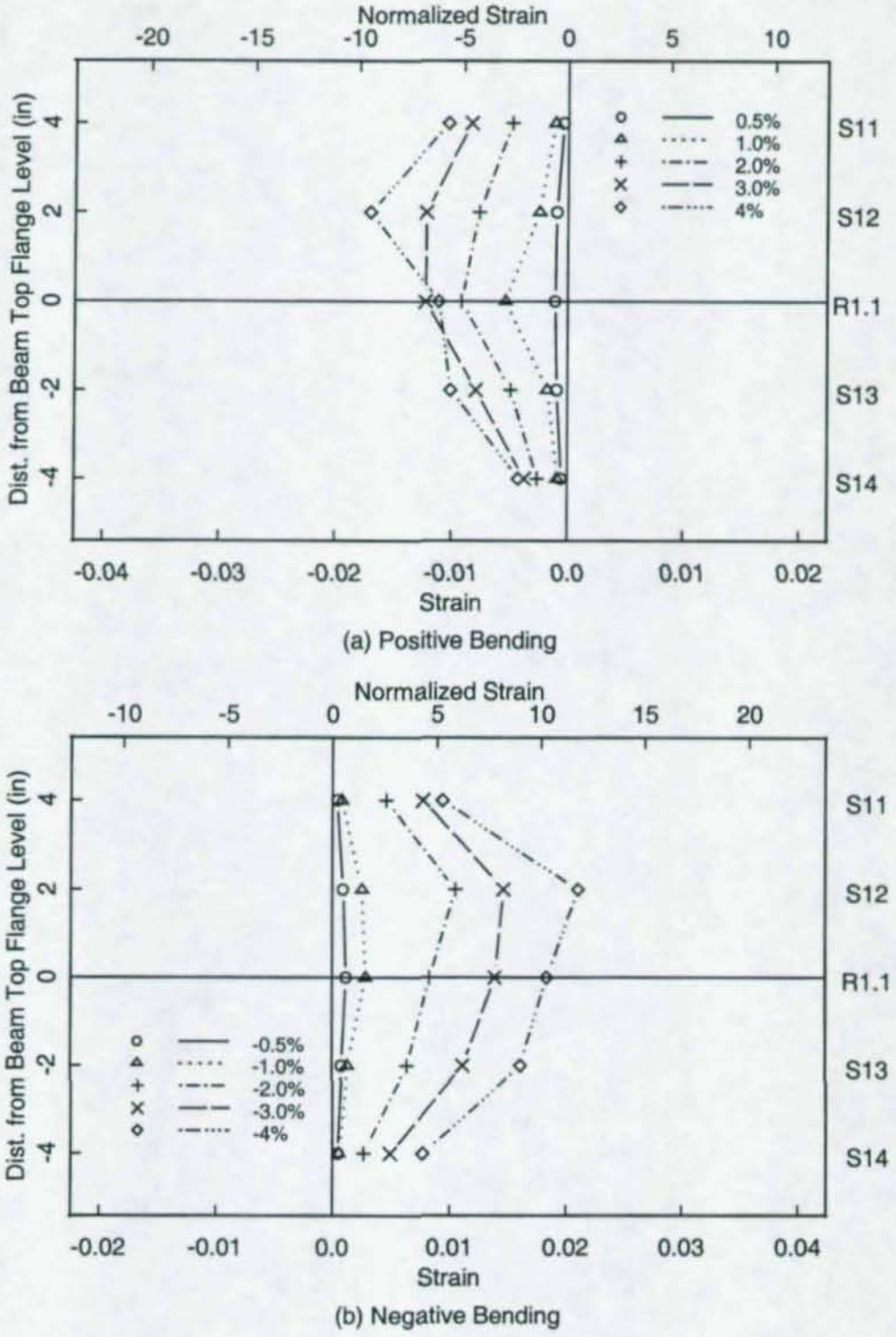

Figure 3.21 Specimen K2: Strain Profiles along Column k Line at Beam Top Flange Level

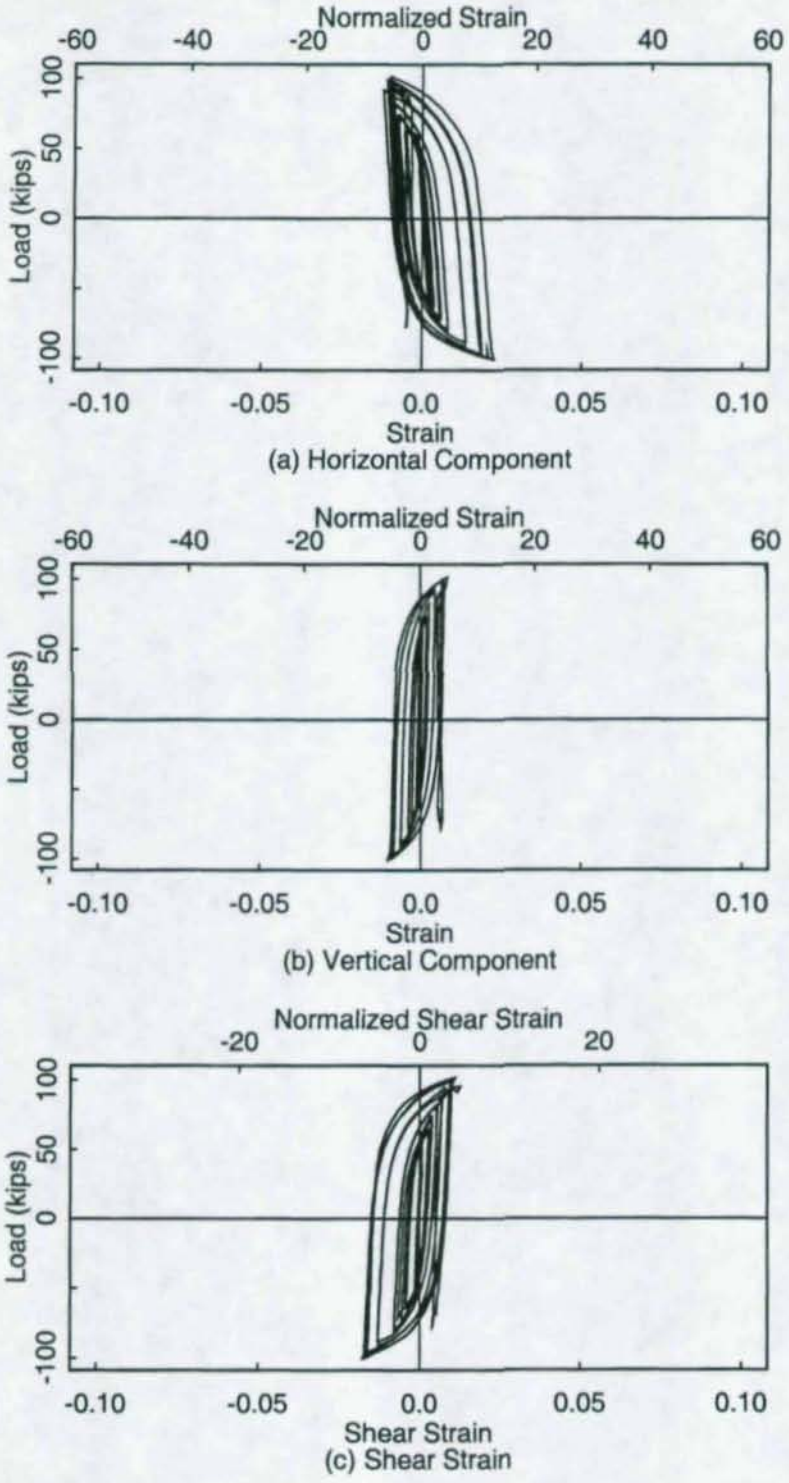

Figure 3.22 Specimen K2: Strains in the Column k Area at Beam Top Flange Level (R1)

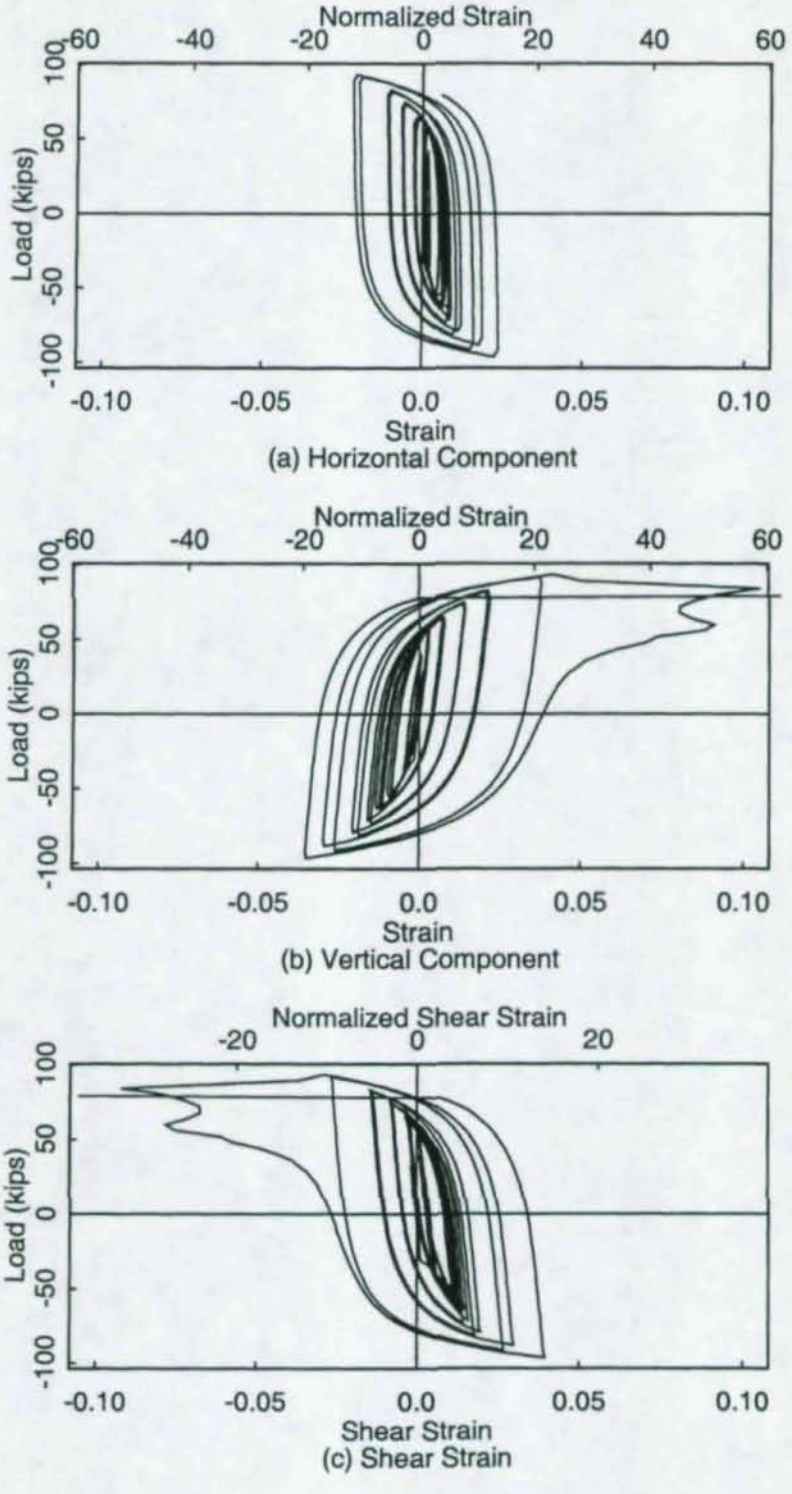

Figure 3.23 Specimen K2: Strains around Hole in the Column k Area (R4)

3.4 Specimen K3 (Non-straightened Column)

Flaking of the whitewash around the hole was observed at 0.5% drift. Panel zone yielding occurred during the 0.75% drift cycles (see Figure 3.24). Flaking of the column flange just above the beam top flange and below the beam bottom flange was noticed at 1.5% drift. Significant column kinking due to the yielding of panel zone occurred at 3% drift (see Figure 3.25). At the end of 3% drift cycles, sign of cracking at the column flange at both beam flange levels were observed.

Figure 3.26 shows the extent of column fracture during the first cycle at 5% drift. Shown in Figure 3.27 is the complete fracture of the column flange during the second cycle of 5% drift. The extent of fracture propagation around the hole during the 5% drift cycles is presented in Figure 3.28. Although the propagation of cracks along the k line was relatively fast, the behavior was not brittle and the strength degradation was limited. The specimen was able to experience one excursion at 6% drift before it failed in the reverse excursion. While the fracture in the column flange propagated into the column web near the k area for Specimens K1 and K2, this was not the case for Specimen K3. The latter one also performed better than the other two specimens; Specimens K1, K2, and K3 experienced complete fracture of the column at 4%, 5%, and 6% drifts, respectively.

The load versus deflection relationship of the test specimen is shown in Figure 3.29. Ignoring the incomplete cycle where column fracture occurred, the total plastic rotation reached 0.04 radian (see Figure 3.30).

The strain profiles across the width of the beam bottom flange are shown in Figure 3.31. The out-of-plane deformation of the column flange reached 0.15 in. at 5% drift [see Figure 3.32(a)]. The strain profiles along the k line of the column at the top flange level are shown in Figure 3.33. Figure 3.34 shows the strain state in the k area at the top flange level. Figure 3.35 shows the strain state next to the hole at the bottom flange level. Because the extent of crack in the hole region of Specimen K3 at 5% drift was more significant than that of Specimen K2 at 6% drift, the softening of the stiffness attracted less force (or strain) demand in the hole region.

Figure 3.24 Specimen K3: Panel Zone Yielding Pattern at 1% Drift

Figure 3.25 Specimen K3: Panel Zone Yielding Pattern at 3% Drift

Figure 3.26 Specimen K3: Column Flange Fracture at Beam Bottom Flange Level (5% Drift, 1st Cycle)

Figure 3.27 Specimen K3: Column Flange Fracture at Beam Bottom Flange Level (5% Drift, 2nd Cycle at 3.14 in)

(a) 5% Drift, 1st Cycle

(b) 5% Drift, 2nd Cycle at 1.02 in

(c) 5% Drift, 2nd Cycle at 3.14 in

(d) 5% Drift, 2nd Cycle at 6 in

Figure 3.28 Specimen K3: Fracture Propagation in Hole Region

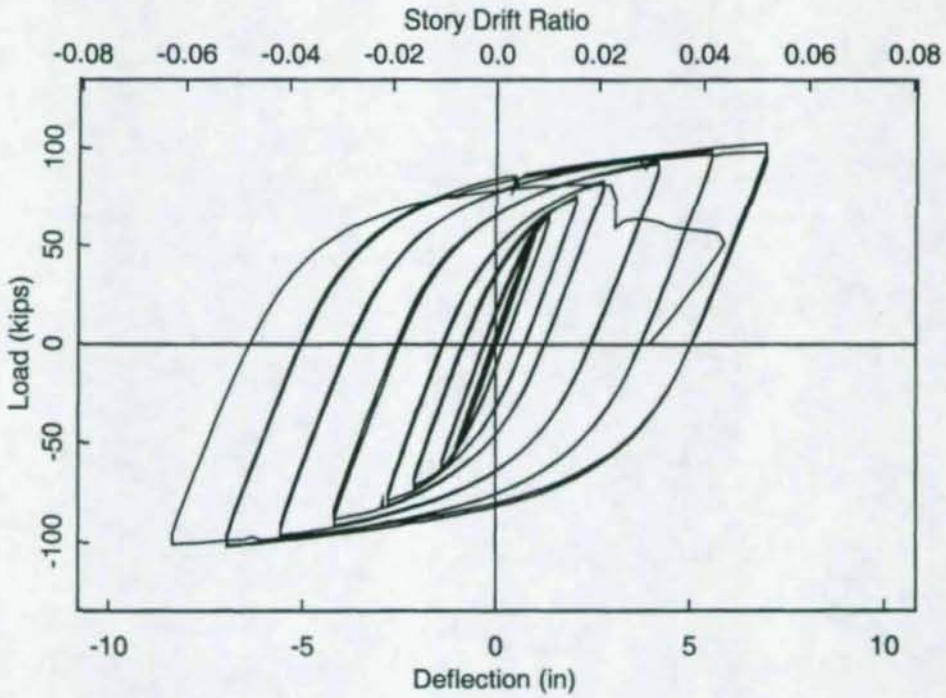

Figure 3.29 Specimen K3: Load versus Beam Tip Deflection Relationship

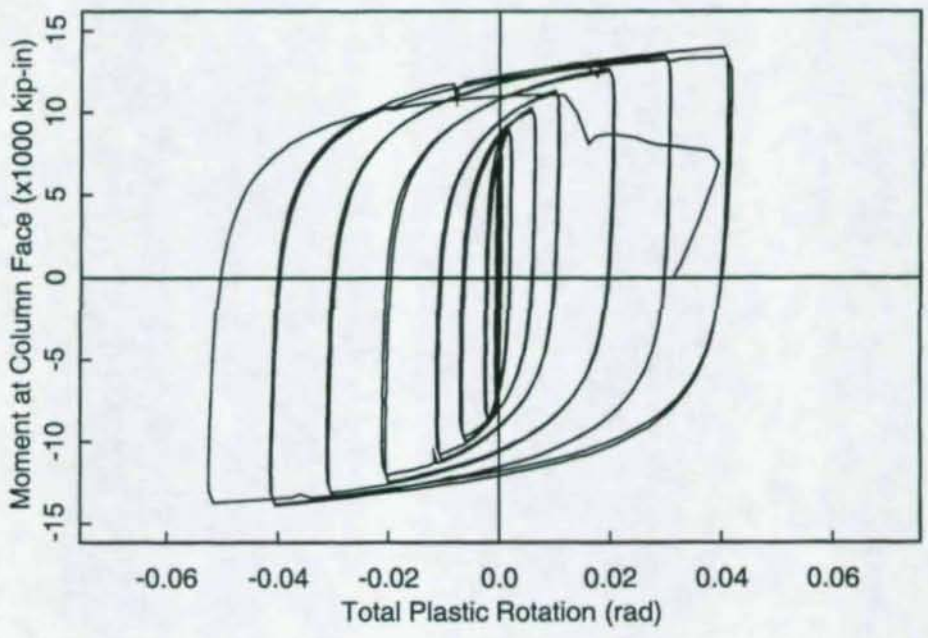

Figure 3.30 Specimen K3: Moment versus Total Plastic Rotation Relationship

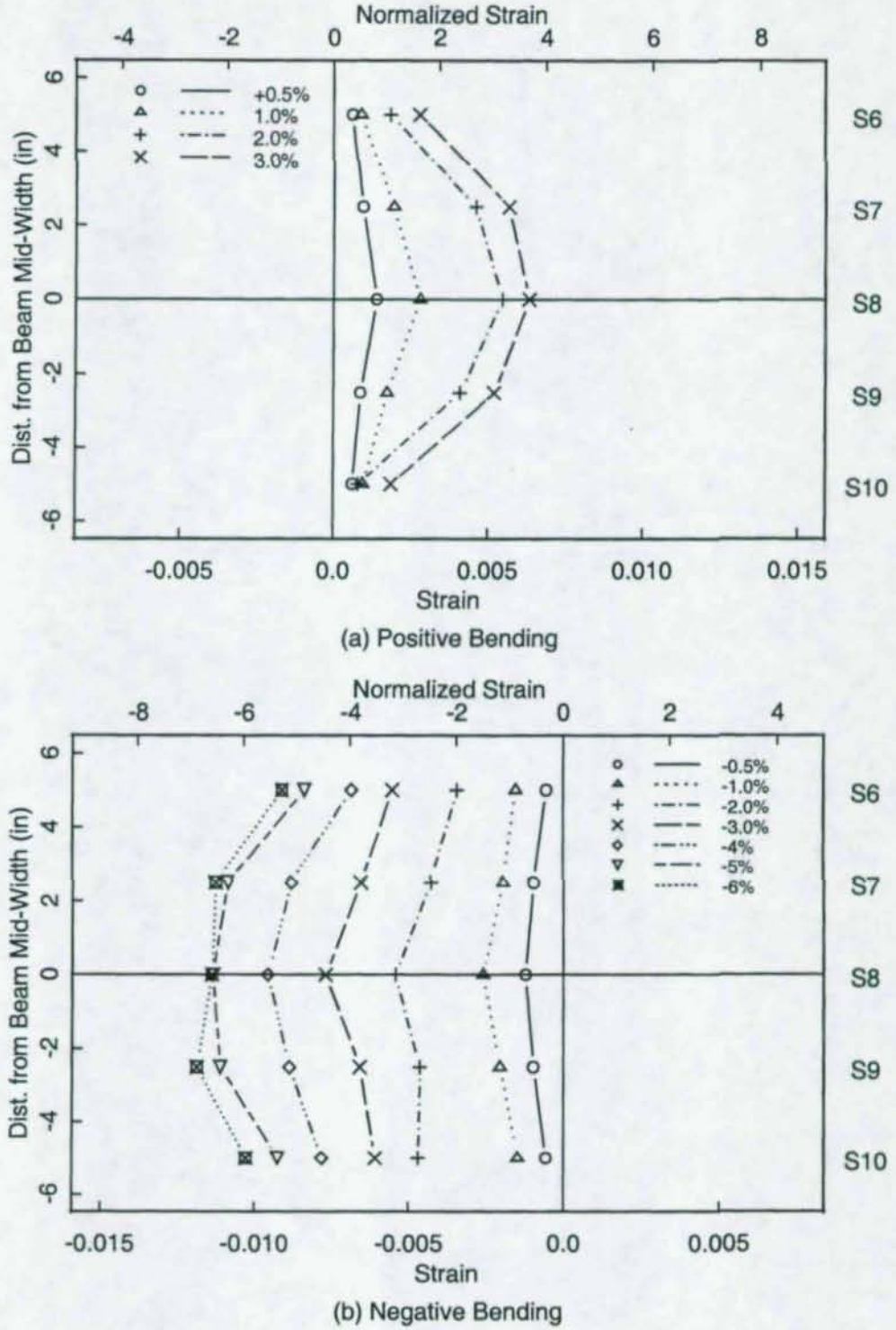

Figure 3.31 Specimen K3: Beam Bottom Flange Strain Profiles

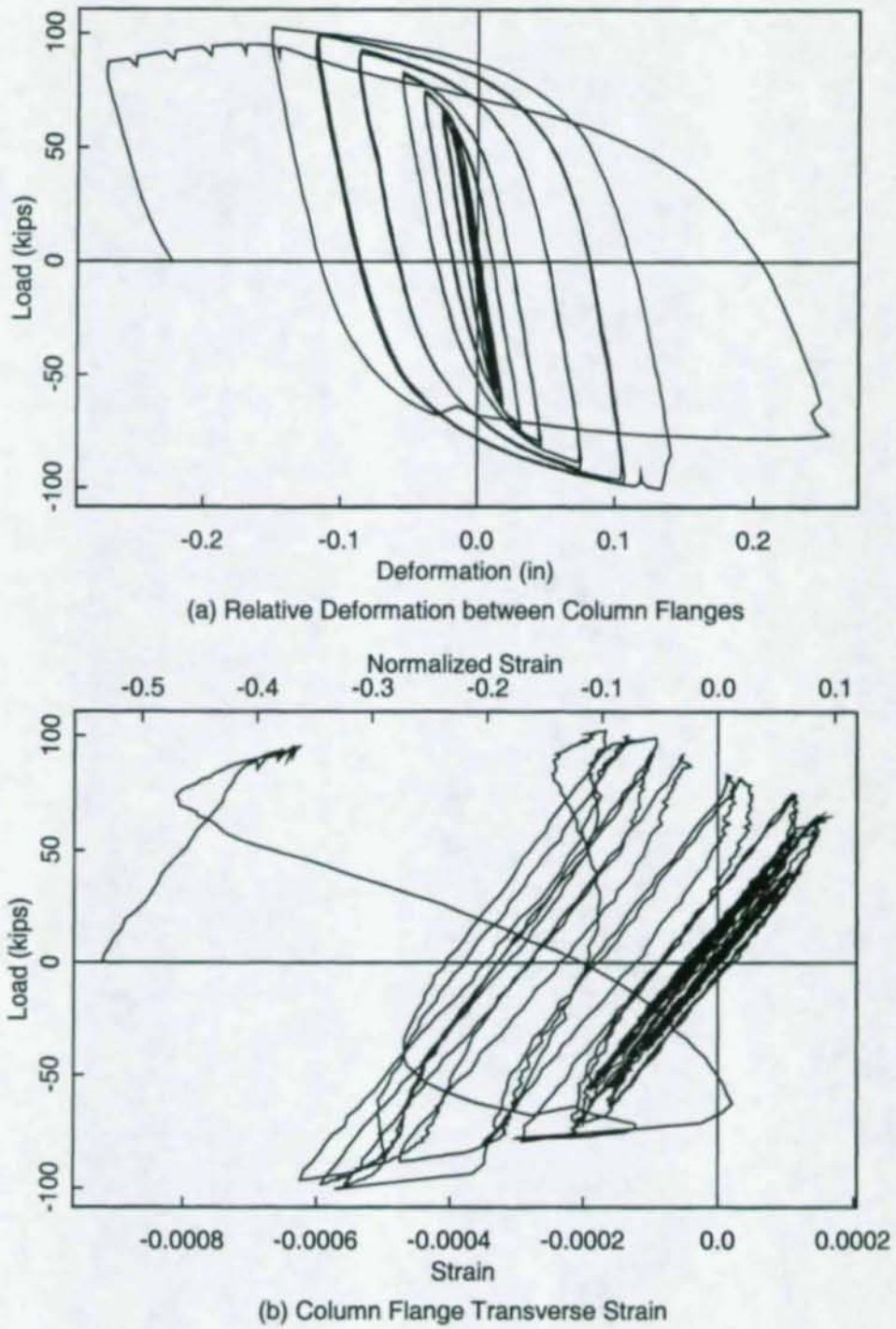

Figure 3.32 Specimen K3: Response of Column Flange Out-of-plane Deformation and Transverse Strain

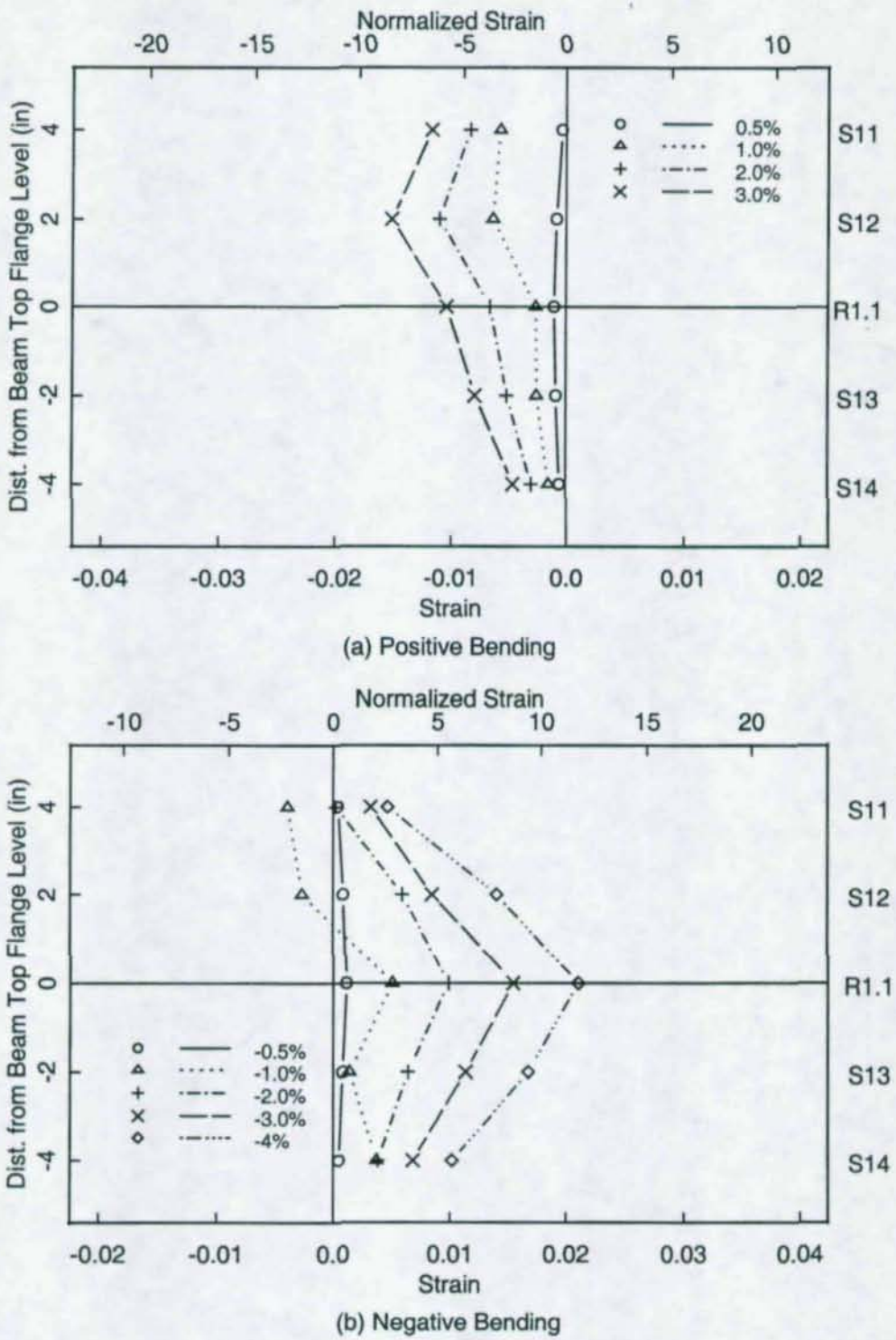

Figure 3.33 Specimen K3: Strain Profiles along Column k Line at Beam Top Flange Level

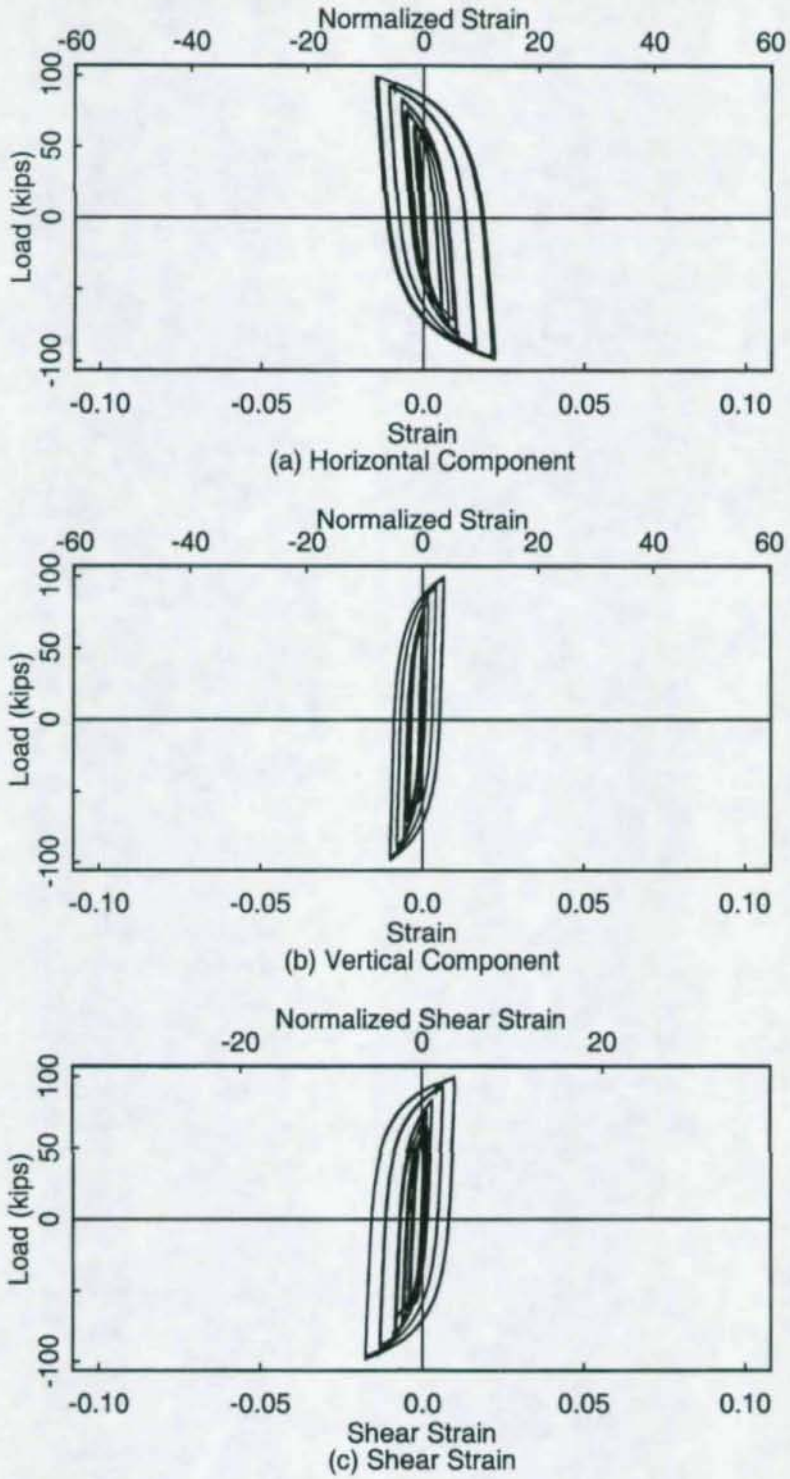

Figure 3.34Specimen K3: Strains in the Column k Area at Beam Top Flange Level (R1)

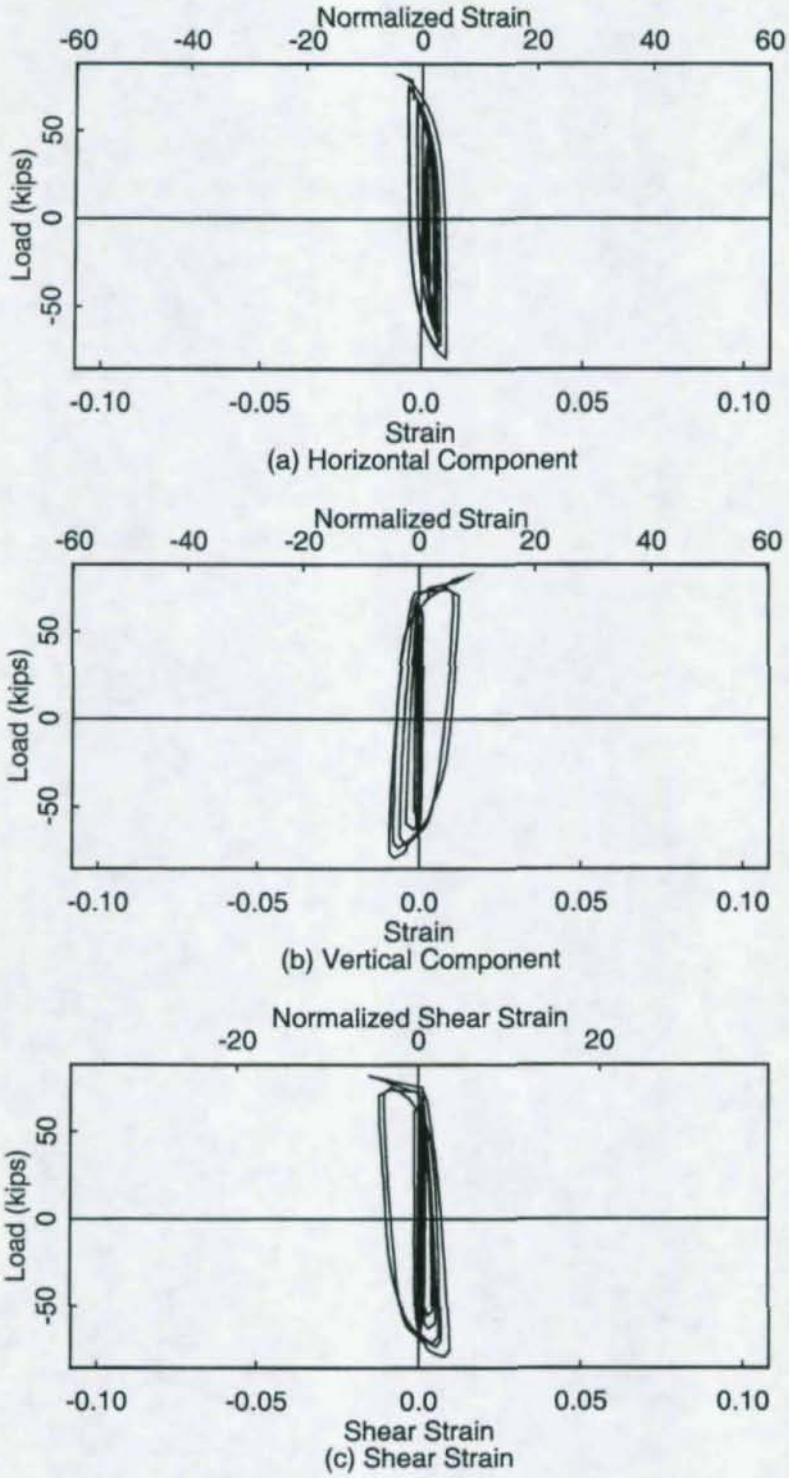

Figure 3.35 Specimen K3: Strains around Hole in the Column k Area (R4)

4. TEST RESULTS OF SPECIMENS WITH CONTINUITY PLATES AND DOUBLER PLATE

4.1 General

Two test specimens to be presented in this chapter were nominally identical to the first three specimens presented in Chapter 3, except that continuity plates and doubler plate were added to enhance the panel shear strength. No attempt was made to avoid welding in the k area of the column.

4.2 Specimen K4 (Rotary-Straightened Column)

Minor flaking of the whitewash in the panel zone (both the column web and doubler plate) was first observed at 1% drift. Flaking in the beam flanges was observed at 3% drift. Figure 4.1 shows that, at 4% drift, the yielding of the test specimen was concentrated in the panel zone. The doubler plate experienced more yielding than that in the column web because a lower grade of steel (A36) was used. Figure 4.2 shows the kinking of the column due to significant yielding in the panel zone during the first cycle at 5% drift. After completing one cycle at 6% cycle, the beam top flange experienced brittle fracture during the second cycle. Figure 4.3 shows that the fracture initiated from the weld access hole in the k area of the beam web and was due to stress concentration. The test was then stopped.

The load versus deflection relationship of the test specimen is shown in Figure 4.4. Prior to column fracture, the total plastic rotation reached 0.047 radian (see Figure 4.5). Figure 4.6 shows that the shear deformations in both the doubler plate and column web in the panel zone were about the same. The continuity plates were effective to reduce the strain concentration in the beam flanges (see Figure 4.7). Nevertheless, continuity plates did not eliminate the strain gradient through the thickness of the beam flange (see Figure 4.8).

(a) Doubler Plate Side

(b) Column Web Side

Figure 4.1 Specimen K4: Yielding of Panel Zone at 4% Drift

(a) Doubler Plate Side

(b) Column Web Side

Figure 4.2 Specimen K4: Column Kinking due to Significant Panel Zone Yielding at 5% Drift

(a) Brittle Fracture of Beam Top Flange

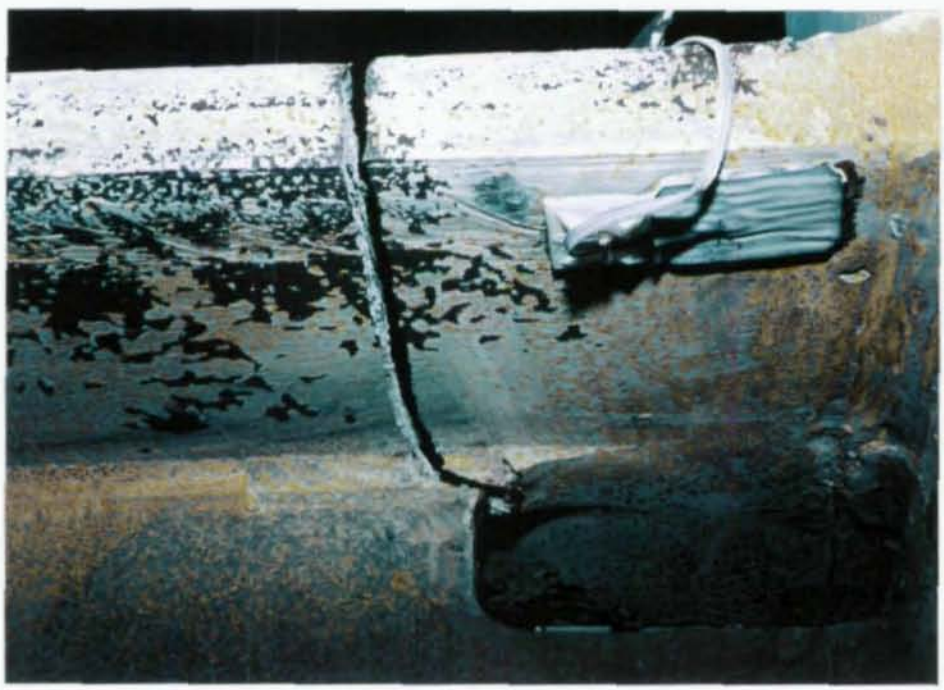

(b) Close-up View of Fracture

Figure 4.3 Specimen K4: Brittle Fracture of Beam Top Flange at 6% Drift

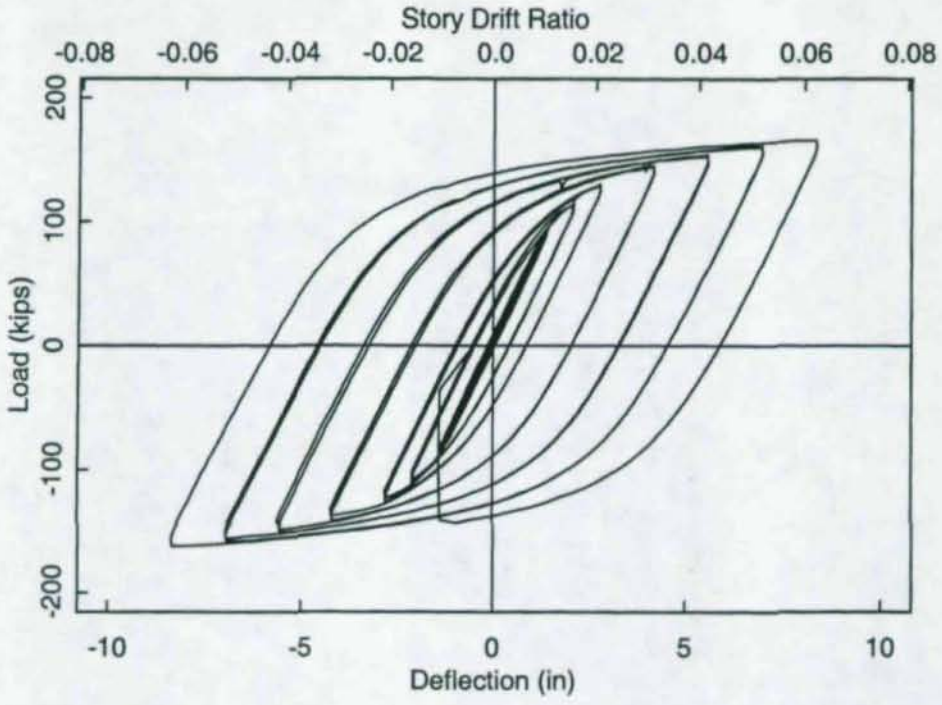

Figure 4.4 Specimen K4: Load versus Beam Tip Deflection Relationship

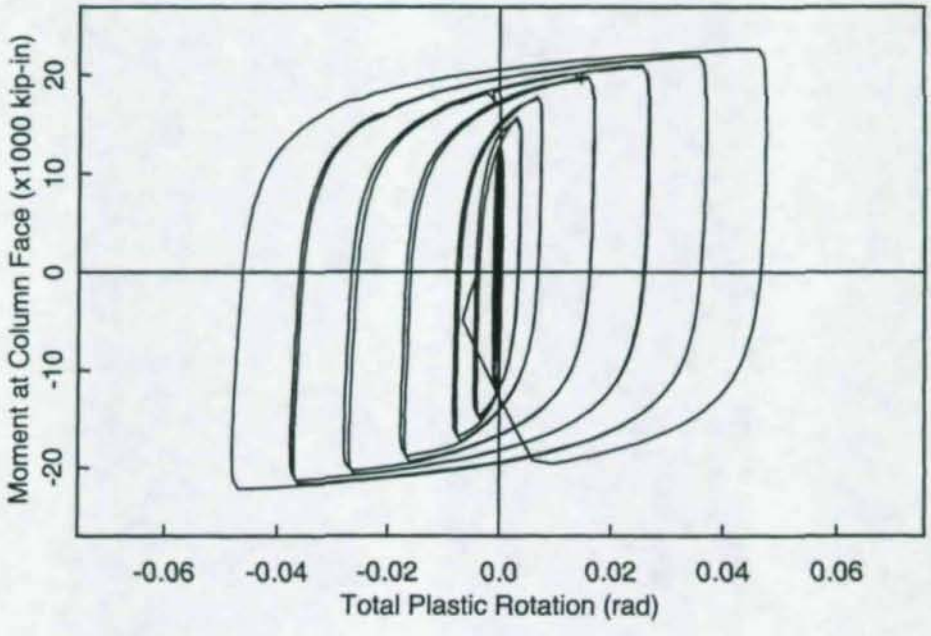

Figure 4.5 Specimen K4: Moment versus Total Plastic Rotation Relationship

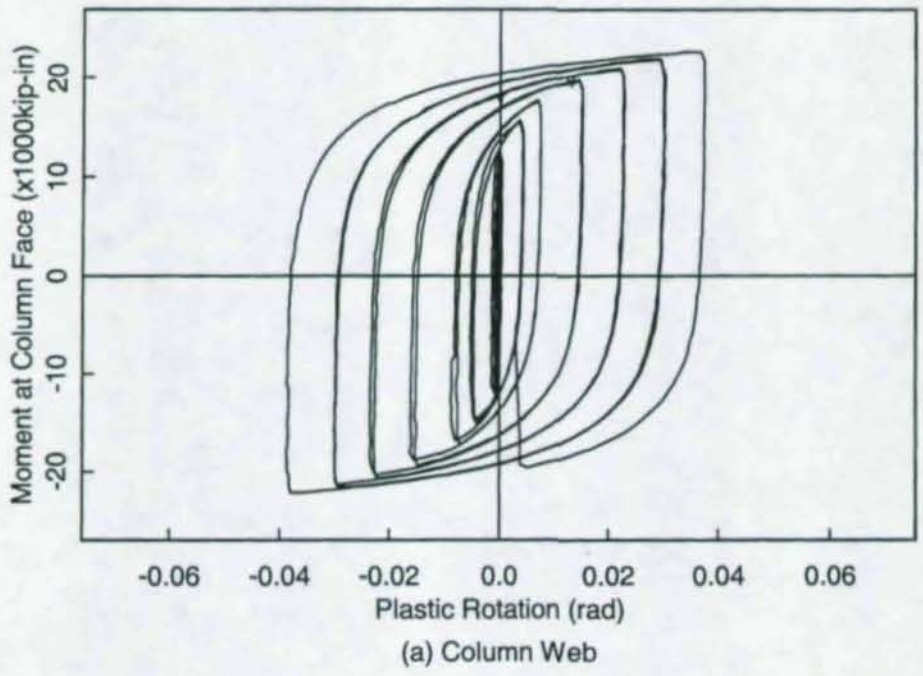

(a) Column Web

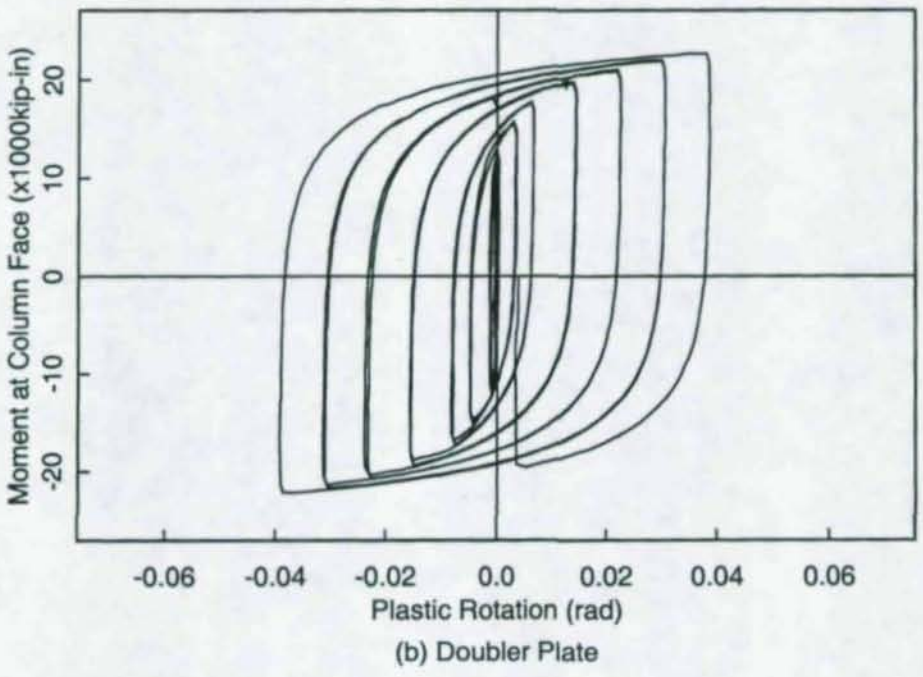

(b) Doubler Plate

Figure 4.6 Specimen K4: Panel Zone Responses

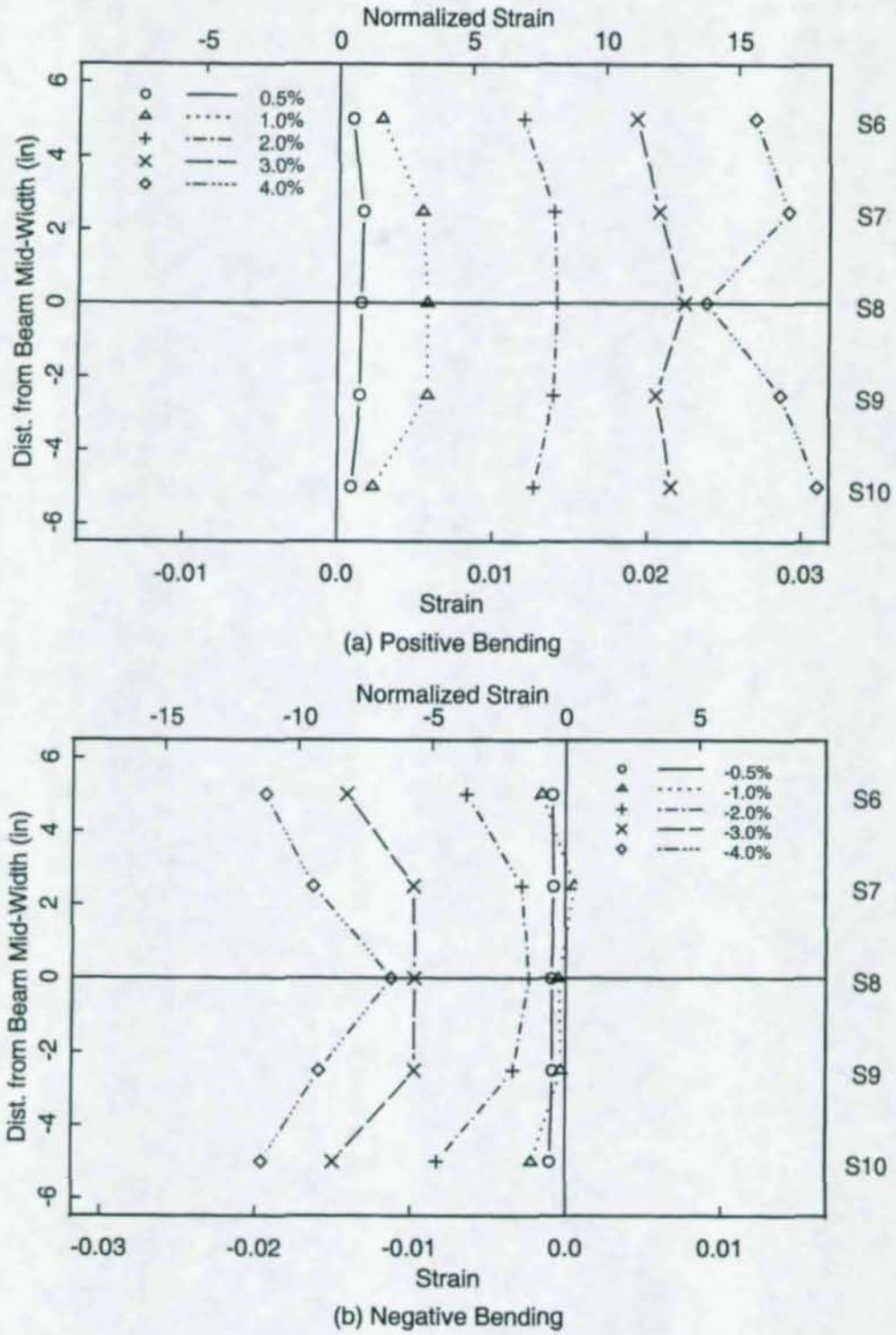

Figure 4.7 Specimen K4: Beam Bottom Flange Strain Profiles

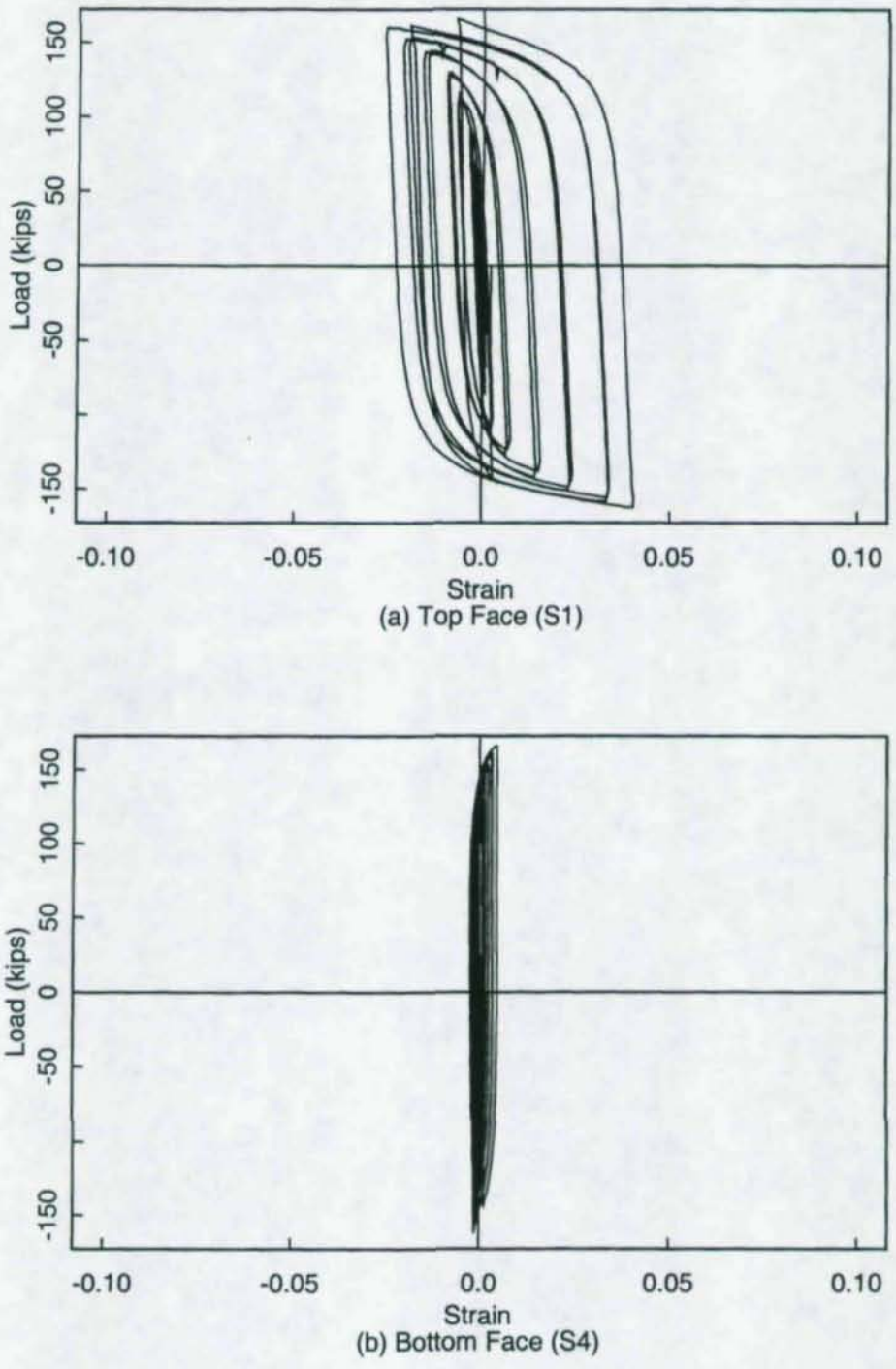

Figure 4.8 Specimen K4: Strain Gradient through Thickness of Beam Top Flange

4.3 Specimen K5 (Non-Straightened Column)

The performance of this specimen was very similar to Specimen K4. Figure 4.9 shows the yielding in the panel zone at 3% drift. Figure 4.10 shows that the beam flange had yielded, but no local buckling was observed. Figure 4.11 depicts the column kinking due to yielding in the panel zone at 5% drift. At this drift level, sign of stress concentration at the weld access hole started to show (see Figure 4.12). The curvature of the beam bottom flange in the weld access hole region, shown in Figure 4.13, was an indication that a significant amount of beam shear was transferred through the beam flanges to the column. Brittle fracture of the beam bottom flange occurred during the first cycle at 6% drift (see Figure 4.14), and the test was stopped. The fracture occurred in the k area of the beam web due to stress concentration in the weld access hole.

The load versus deflection relationship of the test specimen is shown in Figure 4.15. Prior to column fracture, the total plastic rotation averaged 0.038 radian (see Figure 4.16). Figure 4.17 shows that the panel zone shear deformations in both the column web and the doubler plate were similar. With the presence of continuity plates, the beam flexural strains across the width of the beam flange were relatively uniform (see Figure 4.18). A rosette (R3) was placed ½ in. from the weld access hole of the bottom flange. Figure 4.19 shows that the vertical component of the strain reached 7.4 times the yield strain.

(a) Doubler Plate Side

(b) Column Web Side

Figure 4.9 Specimen K5: Yielding Pattern in the Panel Zone at 3% Drift

Figure 4.10 Specimen K5: Yielding in Panel Zone and Beam Flange at 3% Drift

Figure 4.12 Specimen K5: Panel Zone Yielding at 5% Drift

Figure 4.13 Specimen K5: Crack Initiation in Top Flange Weld Access Hole at 5% Drift

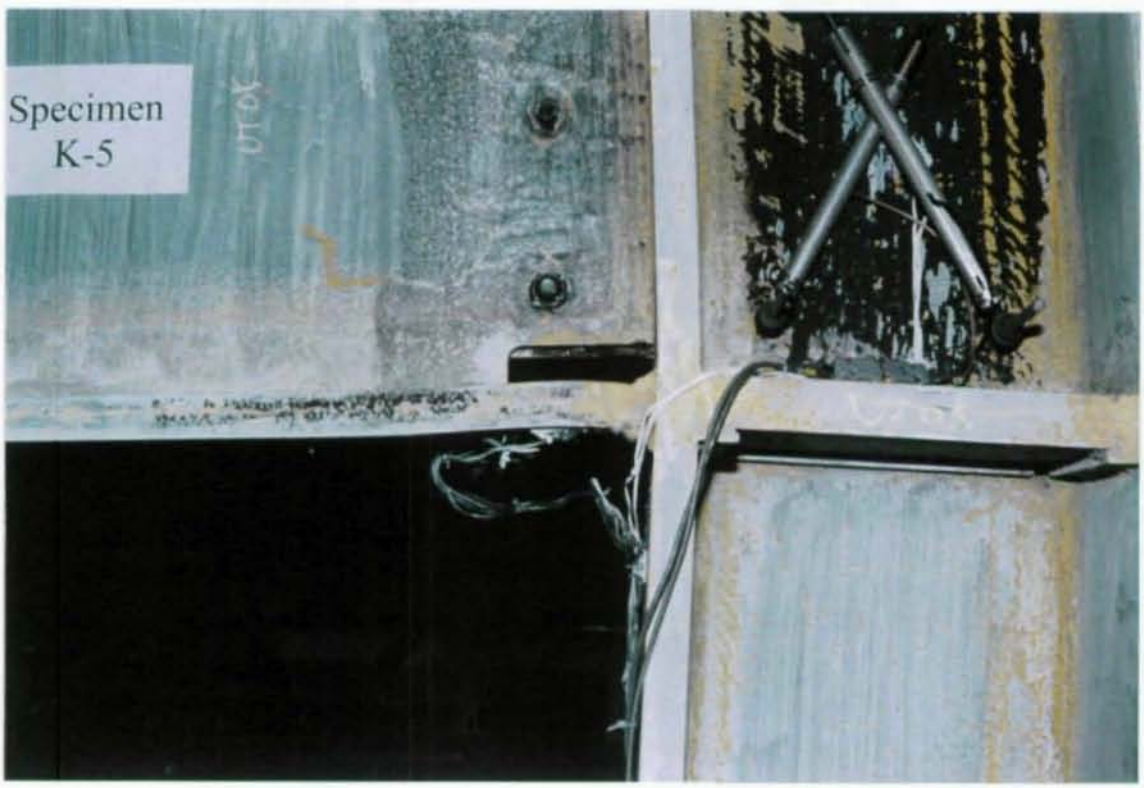

Figure 4.14 Specimen K5: Curvature of Beam Bottom Flange near Weld Access Hole at 5% Drift

(a) Bottom View

(b) Top View

Figure 4.16 Specimen K5: Brittle Fracture of Beam Bottom Flange during the 6% Drift Cycle

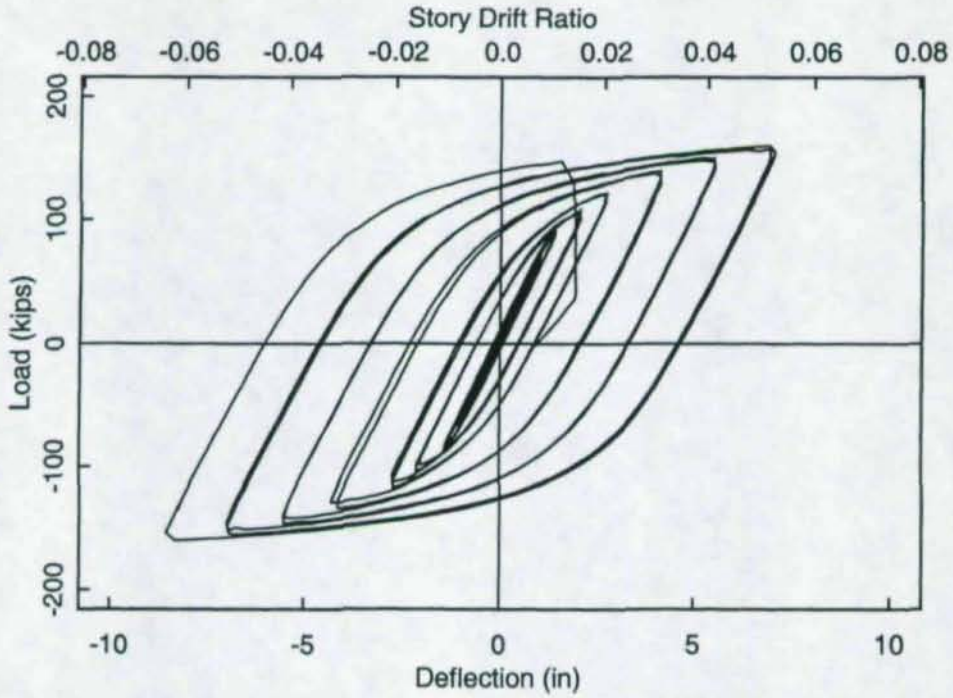

Figure 4.15 Specimen K5: Load versus Beam Tip Deflection Relationship

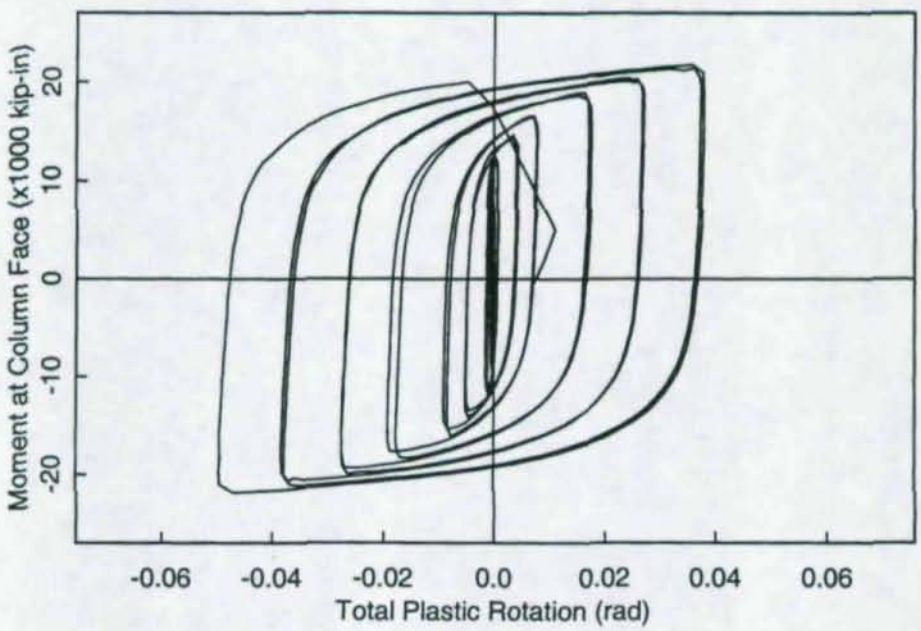

Figure 4.16 Specimen K5: Moment versus Total Plastic Rotation Relationship

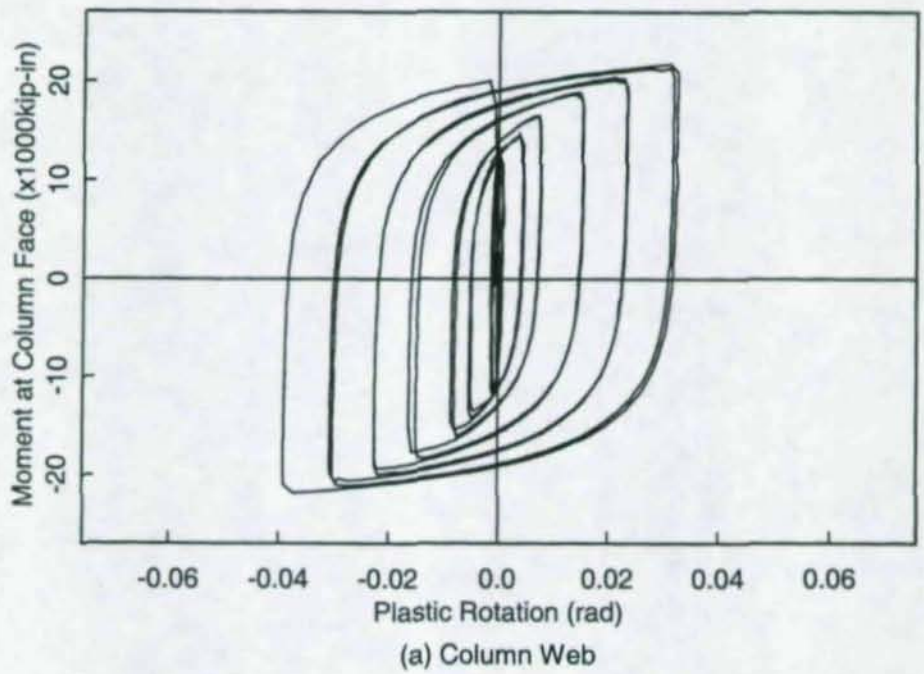

(a) Column Web

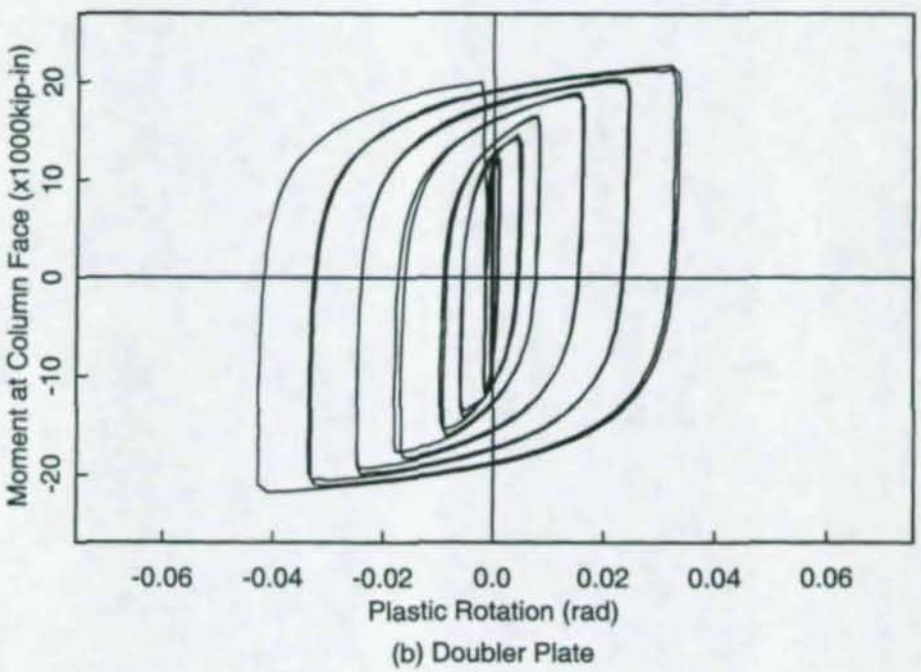

(b) Doubler Plate

Figure 4.17 Specimen K5: Comparison of Panel Zone Responses

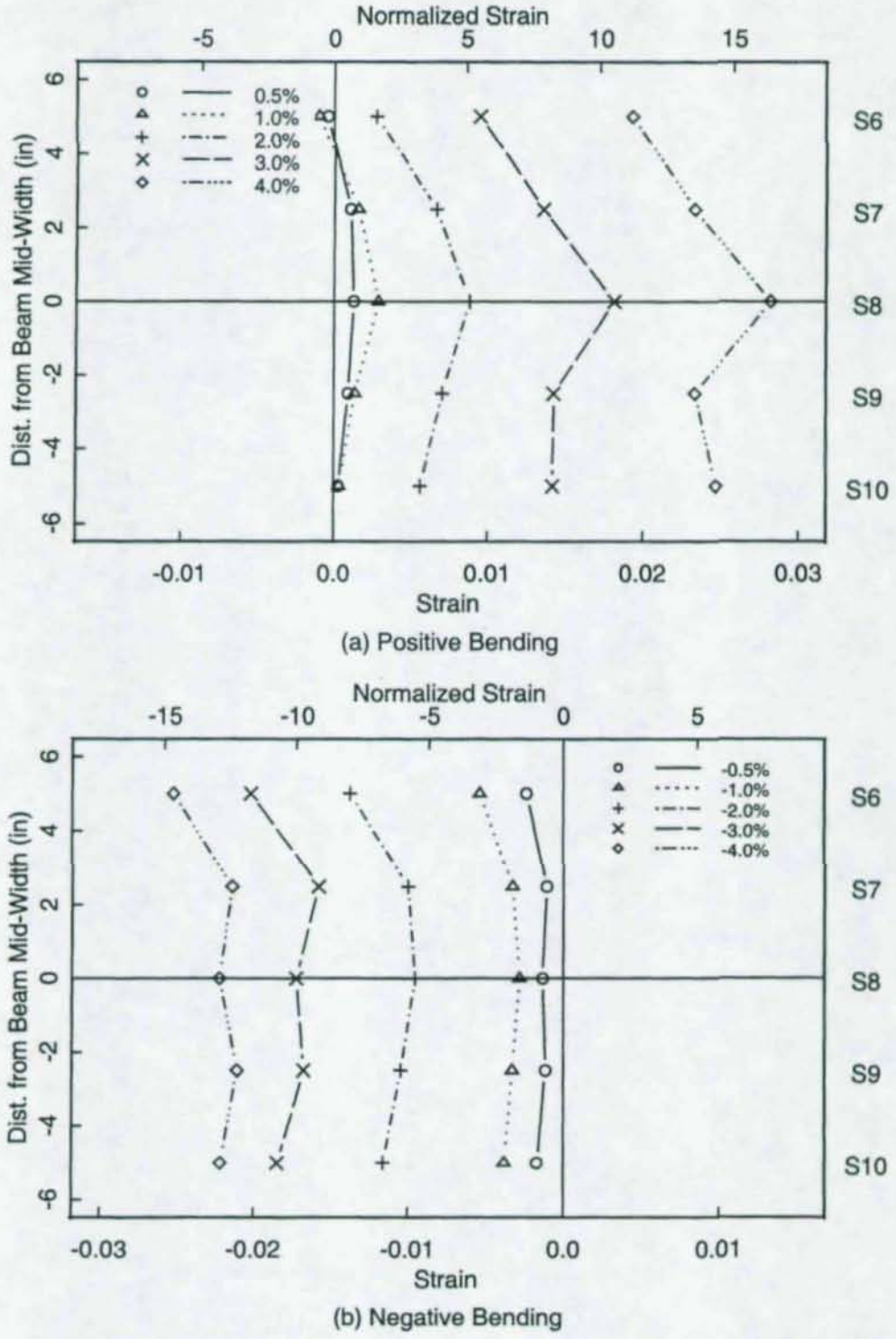

Figure 4.18 Specimen K5: Beam Bottom Flange Strain Profiles

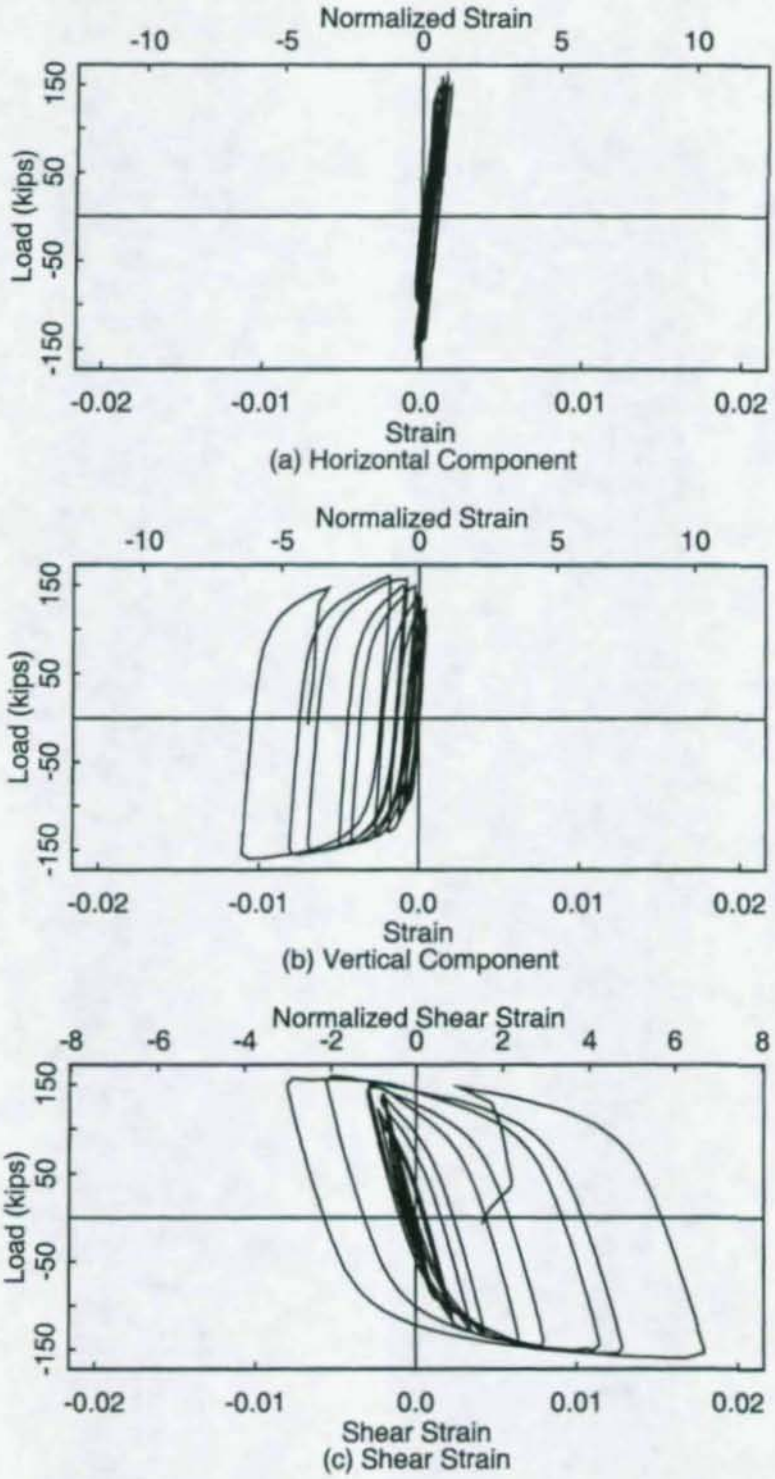

Figure 4.19 Specimen K5: Strains near Beam Bottom Flange Weld Access Hole

5. IMPLICATIONS OF TEST RESULTS

5.1 Test Specimens without Continuity Plates

5.1.1 Failure Mode

All three specimens performed and failed in a similar way. But the presence of the 1-inch diameter drilled hole was not the cause of failure. Significant yielding in the panel zone occurred first. Hairline cracks developed at the toe of the beam flange groove welds at 3% drift; significant kinking of the column flange was also observed at this drift level. Local flange bending of the column produced stress concentration and crack initiation at the center of the column flange. The crack then propagated outward to fracture the column flange across its width. Complete fracture of the column flange occurred at 4% drift for Specimen K1 and 5% drift for Specimens K2 and K3.

5.1.2 k Area Response

Based on the strain gage readings, the maximum strain that developed in the k area at the top flange level of the beam was $24\varepsilon_y$ for Specimen K1 and $12\varepsilon_y$ for Specimens K2 and K3. No fracture was observed at such high strain levels. At the bottom flange level, where a 1-inch hole was drilled, crack did not initiate from the hole in Specimen K1, although crack developed in Specimens K2 and K3 at 5% drift. For the particular connection details and hole arrangement tested, no consistent trend was observed among all three columns.

5.1.3 Plastic Rotation

Although no continuity plates were used, the plastic rotation capacity was 0.02 radian for Specimen K1 and 0.04 radian for Specimens K2 and K3. Because the details and welding of the beam flange groove welded joints were not intended to simulate a field condition, the large plastic rotation should not be construed to imply that continuity plates are generally unnecessary. On the contrary, for the column size tested, the test results clearly showed that local flange bending tends to promote crack development at the toe of the beam flange groove welds.

5.1.4 Strength Comparison

The maximum force applied by the top flange of the beam to the column can be estimated by Eq. 2.3. A comparison of these forces with the LRFD strength (Eq. 2.2) for local web yielding is shown in Figure 5.1. The LRFD strength is exceeded by 34% on average. For seismic design, taking advantage of a portion of this overstrength to reduce the thickness and the associated welding of continuity plates appears beneficial. To match the measured strength for local web yielding, Eq. 2.2 can be modified as follows:

$$R_n = (7k + N)F_{yw}t_w \tag{5.1}$$

5.2 Test Specimens with Continuity Plates and Doubler Plate

The maximum load applied to Specimens K4 and L5 was about 58% higher than those of the first three specimens. Although the beam flanges applied a much higher force to the column, no fracture in the k areas were observed. Both specimens had a weak panel zone, delivering a large plastic rotation capacity (0.038 to 0.047 radian).

Significant kinking of the column due to panel zone yielding did not cause fracture. Instead, since the bending moment in the beam was higher, the beam flange strains ($\approx 15\varepsilon_y$) were about twice the values ($\approx 7\varepsilon_y$) recorded in the first three specimens. Brittle fracture eventually occurred in the beams, initiating at either the top or bottom flange from the weld access hole. Stress concentration that occurred in the k area of the beam was responsible for the crack initiation. To prevent this type of failure, providing a smooth profile for the weld access hole is very important.

Note that the maximum load achieved in Specimens K4 and K5 correlated well with that predicted by Eq. 2.9. The measured response also showed that the panel zone shear deformations in both the column web and the doubler plate were similar.

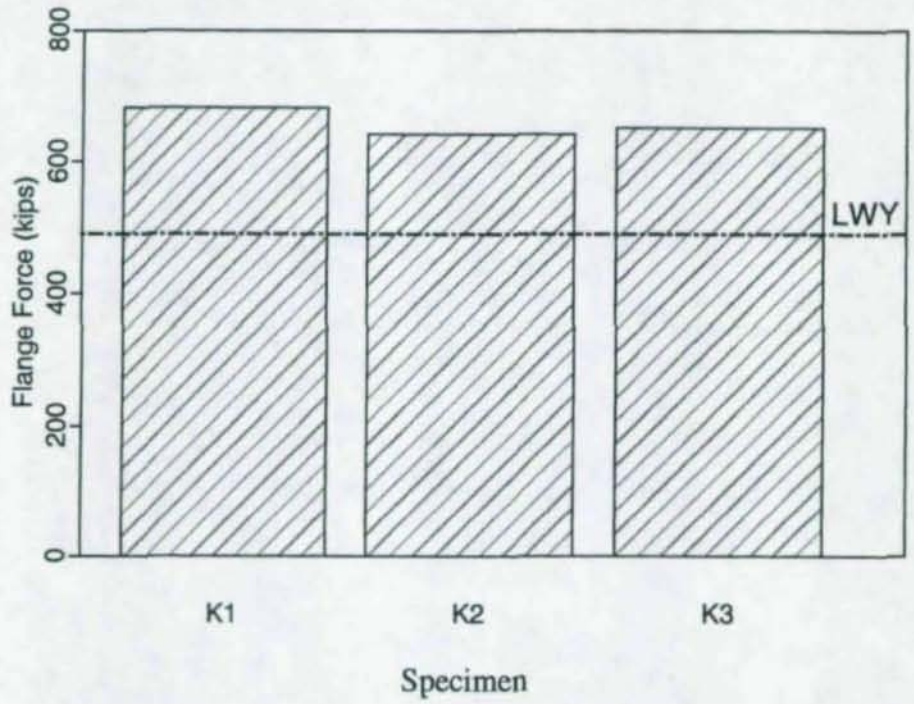

Figure 5.1 Comparison of Strength for Local Web Yielding

6. SUMMARY AND CONCLUSIONS

The research objective was to evaluate the effect of rotary-straightening on the cyclic behavior of k area in rolled column shapes. A total of five full-scale steel moment connections with W14×176 column and W21×166 beam (A992 steel) were tested with the SAC loading protocol. The first three specimens did not use continuity plates and doubler plate; the only variable was the method of straightening of the columns (rotary-straightened, gag-straightened, and non-straightened). To promote the potential for fracture, a 1-in. diameter hole was drilled in the k area of the column at the bottom flange level of the beam. Continuity plates and a doubler plate were used for the last two specimens–one with a rotary-straightened column and the other one with a non-straightened column. No attempt was made to avoid groove welding of the doubler plate and continuity plates in or near the k area. Based on the test results, the following observations can be made.

Maximum strains reached in the k area of the column at the top flange level of the beam were $24\varepsilon_y$ in the rotary-straightened column (K1) and $12\varepsilon_y$ in the gag straightened (K2) and non-straightened columns (K3). No fracture in this area was observed for all three specimens.

A 1-inch hole was drilled in the k area of the column at the bottom flange level of the beam. No crack initiated from the hole in Specimen K1. Cracks did initiated from the hole of Specimens K2 and K3, although this occurred at a high (5%) drift level. For the type of details and member size tested, no consistent trend indicating that a drilled hole would trigger early fracture in the k area of a rotary-straightened column was observed.

The test results showed that, under the cyclic loading condition, the strength as predicted by the LRFD Specification for the limit state of local flange bending and local web yielding is conservative. An average overstrength factor of 1.34 for local web yielding was observed. To reduce the thickness and the associated welding of continuity plates for the seismic design of steel moment connections, it appears desirable to take advantage of a portion of this overstrength.

The plastic rotation capacity varied from 0.02 to 0.04 radian for the first three specimens. Although this modest amount of plastic rotation could be achieved without using the continuity plates, it should be noted that the details and welding of the beam flange groove welds were not intended to simulate a field condition. Without the benefit of continuity plates, the test results clearly showed the potential of crack development in the column flange due to stress concentration from local flange bending.

When continuity plates and doubler plate were used for the last two specimens (K4 and K5), the behavior and failure mode were similar, no matter whether the column was rotary-straightened (K4) or non-straightened (K5). Both specimens experienced brittle fracture of the beam flange at high drift levels ($\geq$ 5%). The fracture initiated from the weld access hole in the k area of the beam, where the transition (i.e., profile) was not made smooth. To prevent this type of fracture, it is essential to provide a smooth transition in the weld access hole. Although both Specimens K4 and K5 had a very weak panel zone, and both specimens were able to deliver large plastic rotations, it should be noted, again, that no attempt was made to simulate a field condition for making the beam flange groove welds.

This testing program did not reveal adverse effect created by rotary straightening. However, material testing conducted by Lehigh researchers (see Figure 2.2 and Figure 2.3) clearly showed that the ductility and toughness of the material in the k area were significantly reduced. Therefore, it is prudent that designers follow the AISC Advisory (Iwankiw 1997) to avoid welding in the k area.

REFERENCES

1. AISC (1994), *Manual of Steel Construction: Load and Resistance Factor Design*, 2nd Edition, Chicago, IL.
2. AISC (1997), *Seismic Provision for Structural Steel Buildings*, 2nd Edition, Chicago, IL, with Supplement No. 1, AISC, Chicago, IL.
3. Brockenbrough, R.L. (2001), "MTR Survey of Plate Material Used in Structural Fabrication," *Final Report to AISC*, R. L. Brockenbrough & Associates, Pittsburgh, PA.
4. Clark, P., Frank, K., Krawinkler, H., and Shaw, R. (1997), "Protocol for Fabrication, Inspection Testing, and Documentation of Beam-Column Connection Tests and Other Experimental Specimens," *Report No. SAC/BD-97/02*, SAC Joint Venture, Sacramento, CA.
5. Dexter, R.J., Hajjar, J.F., Prochnow, S.D., Graeser, M.D., Galambos, T.V., and Cotton, S.C. (2001), "Evaluation of the Design Requirements for Column Stiffeners and Doublers and the Variation in Properties in Properties of A992 Shapes," *Proceedings*, North American Steel Construction Conference, pp. 14-1 to 17-21, AISC, Chicago, IL.
6. Jaquess, T.K. and Frank, K. (1999) "Characterization of the Material Properties of Rolled Sections," *Report No. SAC/BD-99/07*. SAC, Sacramento, CA.
7. Iwankiw, N. (1997), "AISC Advisory Statement on Mechanical Properties near the Fillet of Wide Flange Shapes and Interim Recommendations," *Modern Steel Construction*, Vol. 37, No. 2, AISC, Chicago, IL.
8. Kaufmann, E.J., Metrovich, B., Pense, A.W., and Fisher, J.W. (2001), "Effect of Manufacturing Process on k-Area Properties and Service Performance," *Proceedings*, North American Steel Construction Conference, pp. 17-1 to 17-24, AISC, Chicago, IL.
9. Tide, R. (2000), "Evaluation of Steel Properties and Cracking in "k"-area of W Shapes," *Engineering Structures*, Vol. 22, pp. 128-134.

10. Uang, C.-M. and Bondad, D. (1996), "Static Cyclic Testing of Pre-Northridge and Haunch Repaired Steel Moment Connection," *Report No. SSRP-96/02*, Division of Structural Engineering, University of California, San Diego, CA.